Electrification of Milk Collection Routes

Route-level energy modelling and charging-time feasibility for battery-electric milk collection

Haqvin Wedelsbäck

Independent project in Technology • 15 credits
Swedish University of Agricultural Sciences, SLU
Faculty of Natural Resources and Agricultural Sciences/Department of Energy and Technology
Examensarbete, 2026:1 • ISSN 1654-9392
Uppsala 2026

Electrification of Milk Collection Routes. Route-level energy modelling and charging-time feasibility for battery-electric milk collection

Haqvin Wedelsbäck

Supervisor: Girma Gebresenbet, Swedish University of Agricultural Sciences, Department of Energy and Technology

Examiner: David Ljungberg, Swedish University of Agricultural Sciences, Department of Energy and Technology

Credits:	15 credits
Level:	First cycle, G2E
Course title:	Independent project in Technology
Course code:	EX0874
Programme/education:	Independent course
Course coordinating dept:	Department of Energy and Technology
Place of publication:	Uppsala
Year of publication:	2026
Copyright:	All featured images are used with permission from the copyright owner.
Title of series:	Examensarbete (Institutionen för energi och teknik, SLU)
Part number:	2026:1
ISSN:	ISSN 1654-9392

Keywords: battery-electric truck, milk collection, route energy model, DC fast charging, charging time, charging infrastructure, state of charge, heavy-duty transport

Swedish University of Agricultural Sciences

Faculty of Natural Resources and Agricultural Sciences

Department of Energy and Technology

Abstract

The technical feasibility of electrifying milk collection routes using a battery-electric heavy-duty truck was evaluated by combining reconstructed route data with a physics-based, segment-wise energy model and a time-constrained DC fast-charging model. Event-based trip logs from a Swedish milk haulier were reconstructed into continuous routes using digital maps and elevation data, and each route was discretised into short segments. For each segment, battery energy demand was calculated from rolling resistance, aerodynamic drag, road gradient, kinetic energy changes and auxiliary loads. A time-varying vehicle mass was estimated using a loading model based on farm-level cow numbers, assumed milk yield and pumping capacity. A representative long-range battery-electric truck configuration was assumed with 780 kWh nominal battery capacity and a 10–90% operational state-of-charge (SoC) window. DC fast charging was modelled using a piecewise power–SoC curve and applied at candidate locations with assumed maximum charging powers of 400 kW at depots/dairies (Class 1) and 150 kW at farms (Class 2).

Three representative milk collection routes were analysed. One route was found to be technically feasible within the SoC constraint when high-power charging was applied at the haulier's yard and at the dairy, complemented by opportunistic charging at selected farm stops within available dwell times. For the other two routes, the SoC dropped below the minimum limit before route completion even when charging was allowed at all candidate stops using the full available dwell time; critical points occurred at a Class-2 farm stop for route type 2 and at a non-electrified rest area before the final stretch for route type 3.

It is concluded that electrification potential is strongly route-dependent and that, for more energy-demanding milk routes, feasibility is primarily constrained by charging time availability and achievable charging power rather than by battery capacity alone. Under the optimistic charging assumptions applied in this study—particularly for farm-based charging—full electrification of the most demanding routes would likely require substantial grid reinforcement and/or operational changes such as route redesign, additional vehicles or dedicated intermediate charging hubs.

Keywords: battery-electric truck; milk collection; route energy model; DC fast charging; charging time; charging infrastructure; state of charge; heavy-duty transport

TABLE OF CONTENTS

LIST OF TABLES

LIST OF FIGURES

ABBREVIATIONS

Abbreviation	Meaning
SLU	Swedish University of Agricultural Sciences
BEV	Battery Electric Vehicle
SoC	State of Charge
DC	Direct Current
CCS	Combined Charging System (DC fast charging standard)
GPX	GPS Exchange Format (route file format used by GPX Studio)
SRTM	Shuttle Radar Topography Mission (elevation data source)
OSM	OpenStreetMap (open-source road and map data)

LIST OF SYMBOLS

Symbol	Unit	Description
Route geometry and coordinates		
$\mathrm{lon}_i, \mathrm{lat}_i$	°	Longitude and latitude of point i
x_i, y_i	m	Local Cartesian coordinates of point i
H_i	m	Elevation above sea level at point i
s_k	m	Segment length between points $k$and $k+1$
$d_{xy,k}$	m	Horizontal distance between points $k$and $k+1$
ΔH_k	m	Elevation difference between points $k$and $k+1$
$v_{\max,i}$	km/h	Posted speed limit at point i
$v_{1,k}, v_{2,k}$	m/s	Start and end speed in segment k
$v_{\mathrm{rel},k}$	m/s	Relative air speed in segment k
Δt_k	s	Time spent in segment k
Vehicle and physical parameters		
m_k	kg	Vehicle mass in segment k(truck + trailer + milk)
m_{empty}	kg	Empty mass of truck and trailer (no milk)
g	m/s^2	Gravitational acceleration (9.81 m/s^2)
ρ	kg/m^3	Air density
$C_d A$	m^2	Drag coefficient times frontal area
c_{rr}	–	Rolling resistance coefficient
P_{aux}	W	Auxiliary power (heating, cooling, electronics)
Battery and state of charge		
$E_{\mathrm{batt,nom}}$	kWh	Nominal battery capacity
$E_{\mathrm{batt,usable}}$	kWh	Usable battery capacity (SoC window)
$E_{\mathrm{bat},k}$	J or kWh	Battery energy change in segment k
SoC_k	– or %	State of charge at point/stop k(fraction of nominal capacity)
$\mathrm{SoC}_{\min}$	– or %	Minimum allowed SoC in operation
$\mathrm{SoC}_{\max}$	– or %	Maximum allowed SoC in operation
$\mathrm{SoC}_{\mathrm{taper}}$	– or %	SoC at which DC charging power starts to taper
$\mathrm{SoC}_{\mathrm{target}}$	– or %	Target SoC during charging (e.g. 80–90 %)
Energy model components		
$E_{\mathrm{rull},k}$	J or kWh	Rolling resistance energy in segment k
$E_{\mathrm{aero},k}$	J or kWh	Aerodynamic drag energy in segment k
$E_{\mathrm{hojd},k}$	J or kWh	Height/grade-related energy in segment k(incl. regen)
$E_{\mathrm{kin},k}$	J or kWh	Kinetic energy change in segment k(incl. regen)

Symbol	Unit	Description
$E_{\text{aux},k}$	J or kWh	Auxiliary energy in segment k
$E_{\text{bat,tot}}$	J or kWh	Total battery energy for a route
$\Delta E_{\text{pot},k}$	J or kWh	Potential energy change in segment k
$\Delta E_{\text{kin},k}$	J or kWh	Kinetic energy change in segment k
Efficiencies and recuperation		
η_{drv}	–	Drivetrain efficiency (battery → wheels) during cruise
η_{acc}	–	Effective efficiency during acceleration
η_h	–	Effective efficiency for climbing (height/grade)
n_{regen}	–	Regenerative braking efficiency (fraction of mechanical energy recovered to battery)
η_{ch}	–	Overall charging efficiency (charger + battery)
Charging model		
$P_{\text{DC,max}}$	kW	Maximum DC charging power at a location
$P_{\text{DC}}(\text{SoC})$	kW	DC charging power as a function of SoC
E_{grid}	kWh	Energy supplied from the grid during a charging event
$\Delta t_l^{\text{avail}}$	s or min	Available dwell time for charging at location l
$\mathcal{K}_l$	–	Set of segments between charging location $l$and the next candidate charging point
$E_{\text{req},l}$	kWh	Required battery energy from location $l$to the next critical point
E_{margin}	kWh	Safety margin added to required energy
$\text{SoC}_l^{\text{dep,min}}$	– or %	Minimum SoC required at departure from location l
Load and milk collection model		
$N_{\text{cows},f}$	–	Number of lactating cows at farm f
q_{milk}	L/cow/day	Average daily milk yield per cow
T_{coll}	days	Collection interval (days between collections)
ρ_{milk}	kg/L	Milk density (≈ 1 kg/L)
$V_{\text{milk},f}^{\text{theoretical}}$	L	Theoretical milk volume available at farm f
$V_{\text{milk},f}^{\text{eff}}$	L	Effective milk volume pumped at farm f
r_{pump}	L/min	Milk pump capacity on the truck
$t_{\text{stop},f}$	min	Total stop time at farm f
α_{setup}	–	Fraction of stop time used for setup/non-pumping activities
$t_{\text{pump},f}^{\text{eff}}$	min	Effective pumping time at farm f
$\Delta m_{\text{milk},f}$	kg	Milk mass loaded at farm f
$m_{\text{milk}}^{\text{onboard}}(k)$	kg	Milk mass on board in segment k

1. INTRODUCTION

The decarbonisation of heavy-duty road transport is increasingly prioritised, and battery-electric trucks are being deployed in regional and distribution operations where predictable routes and charging access can be established. For time-constrained logistics, feasibility is determined not only by nominal vehicle range but by the interaction between route-specific energy demand and the time available for charging within normal operations.

Milk collection represents a particularly constrained application. Routes typically include frequent stops, mixed road types and an increasing payload as milk is collected. Charging opportunities are therefore location-dependent and limited by dwell time, which means that electrification feasibility must be assessed by tracking battery state-of-charge along the route and by estimating how much energy can realistically be added during available stops.

In this thesis, the technical feasibility of electrifying selected milk collection routes is evaluated using a physics-based route energy model coupled with a simplified fast-charging representation. Segment-wise route descriptions are used to estimate energy demand and state-of-charge trajectories, and charging requirements are derived under assumed operational constraints. The analysis is used to indicate whether the studied routes can be operated within a defined state-of-charge window and to identify the charging-time and charging-power conditions required for feasible operation.

The report is structured as follows. Section 1 provides context, aim and research questions. The modelling approach and assumptions are described in the Materials and Methods chapter. Results are presented as route energy demand, state-of-charge profiles and charging requirements, followed by a discussion of operational and infrastructure implications and a concluding chapter with recommendations for future work.

1.1 BACKGROUND

Road freight transport is a major contributor to global greenhouse gas emissions and energy use **[1,2]**. Heavy-duty trucks are essential for supplying food, raw materials and consumer goods, but they are still dominated by diesel-powered vehicles **[1,2]**. In parallel, climate targets at EU, national and regional level increasingly require deep emission reductions from the transport sector **[2]**. Battery-electric trucks have emerged as a promising option for decarbonising road freight, particularly for routes with relatively predictable daily patterns and access to suitable charging infrastructure **[3,4]**.

Among these, milk collection logistics represents a specific and operationally important transport task. Raw milk must be collected from a dispersed set of farms and delivered to dairies on a daily basis, under strict time and quality constraints. The vehicles often operate with high gross vehicle weights and follow fixed or semi-fixed routes that repeat from day to day. This combination of heavy loads, rural road networks and repetitive driving patterns makes milk collection an interesting case for studying the feasibility of battery-electric heavy-duty trucks.

At the same time, the adoption of battery-electric vehicles (BEVs) in heavy-duty applications faces several challenges. The energy demand over a route depends not only on distance, but also on road gradient, speed profile, aerodynamic properties, vehicle mass and auxiliary loads. For real-world operations, it is therefore insufficient to rely on simple average energy-per-kilometre values. Instead, route-level energy modelling is needed to capture how topography and driving conditions affect the state-of-charge (SoC) of the battery and the need for intermediate charging **[3,4]**.

In this context, there is a need for practical, yet physically transparent models that can estimate the energy consumption of electric milk collection trucks on specific routes, using data that are realistically available to hauliers and dairies (e.g. GPS logs, digital maps and basic vehicle specifications). Such models can support decisions on vehicle selection, battery sizing and charging strategies, and help identify where electrification is technically feasible within existing operational constraints.

1.1.1 Dairy collection logistics in Sweden

In Sweden, raw milk is typically collected by specialised truck–trailer combinations that operate on pre-defined collection routes. Each route connects a central dairy or depot with a set of farms, often spread over rural areas with a mix of small local roads, regional roads and national highways. The trucks usually start from the depot, visit the farms in a given order, and then return to the dairy for unloading and cleaning before the next shift. **[10]**

The **operating conditions** are characterised by:

- high gross vehicle weights, often in the range of 40–64 tonnes depending on configuration and load;
- a mix of low-speed segments near farms and villages and higher-speed segments on major roads;
- modest but non-negligible variations in elevation, which influence energy use through uphill climbs and downhill regenerative braking;

- relatively fixed daily schedules, where the same or similar routes are repeated over long periods.

Because milk collection is a critical part of the dairy value chain, any electrification strategy must respect time windows for farm collection, hygiene routines, and constraints on maximum route duration. These operational features mean that the **feasibility of battery-electric operation** cannot be assessed purely on distance. Instead, the detailed route profile and energy demand must be examined to ensure that the truck can complete its duties within available battery capacity and charging opportunities.

1.1.2 Electrification of heavy-duty trucks

Battery-electric heavy-duty trucks have developed rapidly in recent years, with increasing battery capacities and higher charging powers becoming commercially available**[3,4].** For regional and distribution transport, several studies have shown that electrification can be technically feasible and, in some cases, economically attractive**[3,4].** However, most existing analyses are based on either simplified driving cycles or aggregated annual energy use, rather than **high-resolution route data** for specific applications such as milk collection.

The energy consumption of a battery-electric truck is driven by several components: rolling resistance, aerodynamic drag, gravitational work against road gradients, changes in kinetic energy due to acceleration and deceleration, and auxiliary loads such as refrigeration or heating. These components depend on route geometry, speed and vehicle parameters. By combining GPS-based route descriptions with a physics-based energy model, it is possible to estimate energy demand at the level of individual route segments and track the evolution of battery SoC along the route**[3,4].**

For dairies and hauliers considering electrification, such route-based models can answer questions such as:

- Can a given electric truck complete a specific milk collection route without intermediate charging?
- If not, where and how much fast charging would be required?
- How sensitive are the results to assumptions about vehicle mass, aerodynamics or auxiliary loads?

This thesis addresses these questions by developing and applying a route-level energy model to a real milk collection route in Sweden, using detailed GPS-based route data and a representative battery-electric truck configuration.

1.2 Aim and research questions

The overall aim of this thesis is to evaluate the technical feasibility of electrifying milk collection routes using battery-electric heavy-duty trucks, by combining detailed route data with a physics-based energy model and a simplified assessment of charging needs and charging infrastructure requirements.

The work uses available digital data sources – such as topographic maps, road network and speed limit data, together with GPS-based route descriptions from transport companies – to construct a segment-wise representation of selected milk collection routes. For each segment, the energy demand of a representative battery-electric heavy-duty vehicle is calculated based

on rolling resistance, aerodynamic drag, road gradient, changes in kinetic energy and auxiliary loads. By tracking the battery state-of-charge between stops, the feasibility of operating the route within existing time constraints can be assessed.
In addition, the model is used to estimate the **location, power and energy requirements for fast charging** along the route, given assumptions about the chosen vehicle, charger technology and operational constraints. This allows a first assessment of whether suitable high-power chargers would be needed away from depots, and what implications this might have for the local electricity grid and energy supply.
The study focuses on a truck configuration that is representative of current or near-future battery-electric heavy-duty vehicles, using technical specifications from manufacturers and values from the scientific literature where detailed data are not publicly available**[3–5]**.
Based on this, the thesis addresses the following research questions:

1. **Route energy and SoC:**
What are the segment-wise energy demand and resulting battery SoC trajectories for the selected milk collection routes when a representative long-range battery-electric truck configuration is assumed (including route topography, speed limits, auxiliary loads, and a time-varying vehicle mass due to milk loading)?
2. **Time-constrained charging feasibility at operational stops:**
When charging is allowed during operational stops, and charging power is determined using a literature-based DC charging curve, is sufficient energy added within the available dwell times to complete each route within the SoC constraint?
3. **Infrastructure requirements and bottlenecks under optimistic assumptions:**
Under plausible but optimistic assumptions for charging infrastructure availability (e.g., high-power charging at depot/dairy and limited fast charging at farms), which routes are technically feasible or infeasible, and to what extent is feasibility limited by charging time and charging power (i.e., infrastructure) rather than by battery capacity alone?

By answering these questions, the thesis aims to provide a transparent, route-specific assessment of when and how battery-electric trucks can be deployed for milk collection, and to identify potential operational adaptations.

1.3 Scope and limitations

This thesis focuses on the technical feasibility of operating selected milk collection routes with a battery-electric heavy-duty truck, based on physics-based energy modelling and simplified charging analysis. The work is deliberately limited in scope and makes several assumptions, which should be kept in mind when interpreting the results.
First, the energy model is built on standard vehicle dynamics and uses a simplified representation of the main energy-consuming components: rolling resistance, aerodynamic drag, gravitational work against road gradients, changes in kinetic energy and auxiliary loads. The model is applied to a discretised representation of the route, based on GPS-derived points and external elevation and speed limit data. Because the model does not use time-resolved speed measurements, but relies primarily on posted speed limits and smoothed elevation

profiles, the resulting energy use and state-of-charge (SoC) profiles should be seen as approximations rather than exact reconstructions of real driving. The model also neglects very short low-speed movements on farms and yards; each farm is represented by a point on the public road network, and manoeuvring on internal farm roads is not modelled explicitly. Wind is not treated dynamically: in the base case, the relative air speed is taken as the vehicle speed (zero wind), so variations due to head- or tailwinds are not captured.

Second, several input parameters are based on assumptions and literature values. Detailed manufacturer data for the chosen battery-electric truck configuration are not fully available in the public domain, especially for vehicles that are still under development. Instead, the model uses a combination of indicative manufacturer specifications and parameter values taken from scientific literature and technical reports**[3–5]**. This applies, for example, to the effective drag area, rolling resistance coefficient, drivetrain efficiencies and auxiliary power demand. Auxiliary loads are represented by a constant auxiliary power of 10 kW, intended to cover cab heating/cooling, onboard systems and cooling of the milk in the tank. The electrical power required to drive the milk pump during loading is assumed to be negligible compared to traction power and is not modelled explicitly**.** In reality these loads vary with season, ambient temperature and operating conditions, so the model may underestimate auxiliary energy use in, for example, cold winter operation. While the chosen values are considered reasonable for a modern heavy-duty vehicle, they introduce uncertainty into the absolute energy estimates.

Third, the route sample analysed in this thesis is limited. The study examines one (or a small number of) specific milk collection route(s) provided by a particular transport company. These routes are shaped by the company's current logistics planning, farm locations and dairy locations, and are not intended to represent a statistically general "average" milk collection route. The conclusions are therefore most directly applicable to the studied route(s) and should be generalised to other regions or operators only with caution.

Fourth, the analysis is restricted to technical feasibility in terms of energy use, SoC trajectories and basic charging requirements. The thesis does not include a detailed assessment of economic feasibility, business models, regulatory aspects or organisational willingness to invest in electrification. Likewise, the grid and energy supply aspects are treated at a simplified, order-of-magnitude level: the study estimates required charging power and energy at candidate locations but does not perform detailed power flow calculations, grid reinforcement studies or cost analysis for network upgrades.

Fifth, the treatment of vehicle mass and loading is simplified, although the mass is not assumed to be constant. Instead, the truck mass is varied along the route using an approximate loading model for raw milk. The model assumes that farms are normally collected every second day, that the average milk production per lactating cow is 30 L/day, and that milk density and pumping capacity are constant. The number of lactating cows per farm is estimated from publicly available information, such as farm websites or newspaper articles. Pumping times are not directly available in the route data and are therefore inferred from assumed setup times, tank capacity and the requirement that the tank must be full and return to the dairy at the appropriate point in the route. This approach provides a reasonable first estimate of the mass after each farm stop, but it does not capture short-term variations in milk

yield, herd size changes, on-farm storage practices or operational deviations from the assumed collection pattern.
Finally, the qualitative insights from stakeholder interviews are based on a limited number of respondents and are used primarily to provide context and to inform realistic assumptions about operations and charging opportunities**[10].** The interview material is not intended to be statistically representative of the entire dairy or transport sector.
Within these boundaries, the thesis aims to provide a transparent and physically grounded assessment of the energy demand and charging needs for the selected milk collection routes, and to illustrate how such route-level modelling can support early-stage decisions about the electrification of similar transport tasks.

2. MATERIALS AND METHODS

2.1 Route data from the transport company

The primary route data used in this thesis were provided by the milk haulier **Mejeritransporter Karlstad**. The company kindly supplied trip logs for a representative milk collection route. The logs were not continuous GPS traces, but **event-based records** in tabular form, containing for each event:

- date and time,
- event type (Start / Stop),
- distance driven since the previous event and accumulated distance,
- driving time and accumulated driving time,
- stop duration and accumulated stop duration,
- a textual position (road name, town),
- and a **Google Maps link** to the location of the start or stop.

Thus, the data describe when and where the truck started and stopped, and how far and how long it had driven between those points, but they do not include a full sequence of intermediate coordinates.

To reconstruct a continuous route suitable for energy modelling, the Google Maps links for each start and stop were used to extract the corresponding coordinates. These coordinates were then imported into **GPX Studio** as waypoints, in the order they appear in the trip log [9]. GPX Studio was used to automatically route along the existing road network between each pair of consecutive waypoints, creating a continuous polyline that follows the most plausible road connection between the recorded start and stop locations.

The resulting routed trip was then exported from GPX Studio as a GPX file. This file contains a dense sequence of points along the reconstructed route, which serve as the basis for the subsequent energy calculations. Obvious duplicates and non-relevant segments were removed so that the final file represents a single, cleaned reference trip.

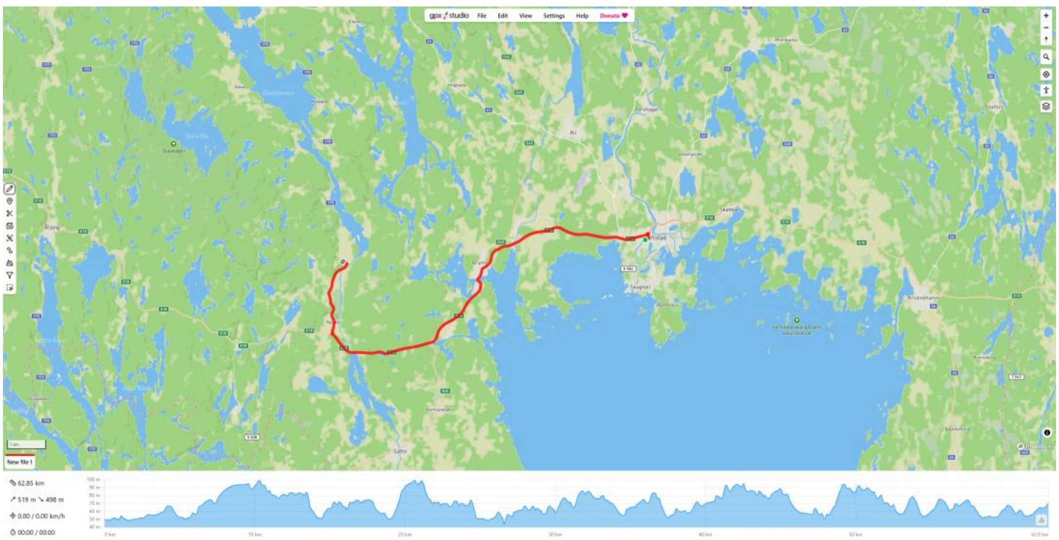

Figure A. Reconstructed milk collection route in GPX Studio, based on start/stop positions from the haulier's trip log. The lower panel shows the corresponding elevation profile along the route.

2.1.1 Elevation, road class and speed limits

When exporting the reconstructed route, GPX Studio was configured to include additional attributes for each point along the polyline. In particular, GPX Studio queries open data sources such as the **Shuttle Radar Topography Mission (SRTM)** for elevation and uses the underlying digital road network (e.g. OpenStreetMap) for road type and posted speed limits [6,7].

For each point along the routed trip, the exported GPX file therefore contains:

- longitude and latitude,
- elevation above sea level (ele_m),
- road class,
- and posted speed limit (maxspeed_kmh).

These points were then converted to a text or CSV format and lightly cleaned (removing artefacts and ensuring consistent point spacing), resulting in a list of "measurement points" along the route. This list, consisting of lon, lat, ele_m and maxspeed_kmh for each point, is the primary input to the MATLAB energy model used in this thesis.

```
"lon=0.001217, lat=0.002539, maxspeed_kmh=70, ele_m=55.5"
"lon=0.002372, lat=0.002216, maxspeed_kmh=70, ele_m=55.5"
"lon=0.00302,  lat=0.002023, maxspeed_kmh=70, ele_m=56"
"lon=0.003701, lat=0.001811, maxspeed_kmh=70, ele_m=57.25"
"lon=0.004084, lat=0.001681, maxspeed_kmh=70, ele_m=57.75"
"lon=0.004544, lat=0.001507, maxspeed_kmh=70, ele_m=59.5"
"lon=0.004997, lat=0.001301, maxspeed_kmh=70, ele_m=61.5"
"lon=0.00552,  lat=0.001059, maxspeed_kmh=70, ele_m=62.25"
"lon=0.005838, lat=0.000898, maxspeed_kmh=70, ele_m=62.5"
```

Figure B. *Example of the processed route file used as input to the energy model. Each row corresponds to one point along the route and includes longitude, latitude, posted speed limit and elevation.*

2.2 Vehicle and powertrain

The energy model is built around a heavy-duty milk collection vehicle representative of current Swedish practice, but implemented as a battery-electric truck–trailer combination. Conventional diesel operation is used only as a qualitative reference for typical gross vehicle masses and milk tank/pump capacities; no quantitative fuel consumption model is included.

2.2.1 Selection of reference BEV and data sources

The battery-electric truck configuration in this thesis is inspired by current and near-term long-range heavy-duty BEVs that were highlighted by the haulier during interviews. In particular, a recently announced long-range Volvo electric truck with an advertised range of up to 600 km per charge was used as a reference for overall size and battery capacity [5] . The studied vehicle is not intended to be an exact model of this specific truck. Instead, limited publicly available manufacturer data (e.g. gross combination weight, indicative battery capacity and charging power) were used where possible, and complemented with generic parameter values from scientific literature, field studies and other electric heavy-duty vehicles when data were missing. The resulting parameter set is therefore meant to represent a generic long-range battery-electric heavy-duty truck capable of completing the longest studied milk collection route on a single charge, rather than a detailed simulation of a particular commercial model.

2.2.2 Battery-electric reference truck configuration

The main vehicle considered in the model is this generic battery-electric truck–trailer combination, parameterised to be realistic for long-range Swedish milk collection.
The key parameters used in the energy model are:

- **Gross vehicle mass** m: a nominal fully loaded mass of $m = 55\ 000\ kg$ is used, consistent with typical Swedish milk collection combinations. Along the route, the vehicle mass is varied according to the loading model in Section 2.1.5, based on estimated milk volume at each farm.
- **Aerodynamic properties**: the product of drag coefficient and frontal area is set to $C_d = 6.7\ m^2$representative of a streamlined heavy-duty tractor with a high trailer.
- **Rolling resistance**: the rolling resistance coefficient is set to $c_{rr} = 0.006$, a typical value for fully loaded heavy trucks on paved roads.
- **Driveline efficiencies**: average efficiencies are used to link wheel-level energy to battery-level energy. A generic driveline efficiency $\eta_{\text{drv}} = 0.92$ is applied for constant-speed operation, while $\eta_{\text{acc}} = 0.92$ and $\eta_h = 0.92$ are used for acceleration and uphill driving, respectively. Regenerative braking efficiency is set to $n_{\text{regen}} = 0.70$, capturing losses in the electric machine, inverter and battery during energy recovery.
- **Battery capacity and usable window**: the nominal battery capacity is chosen to be in the same range as Volvo's long-range electric trucks (around 700–800 kWh). In the model, a specific value $E_{\text{batt,nom}}$(e.g. 780 kWh) is assumed. Only a defined SoC window (e.g. 10–90 %) is treated as usable in operation, to reflect battery lifetime constraints.
- **Auxiliary power**: auxiliary loads (cab heating/cooling and onboard systems) are represented by a constant auxiliary power P_{aux}. In the base case, $P_{\text{aux}}$is set to a low value or zero to focus on traction energy; sensitivity cases can be defined with higher auxiliary loads.

These parameters define the physical input to the segment-wise energy model in Section 2.3. For each segment, the model computes the traction energy required at the wheels and converts it to battery energy by applying the efficiencies above. Regenerative braking is modelled by allowing a fraction $n_{\text{regen}}$of the kinetic and potential energy released during downhill and deceleration phases to be returned to the battery.
To emphasise generality, the results are presented in terms of energy per route and per kilometre, rather than as performance of a specific commercial model. The chosen parameter values should thus be interpreted as one plausible realisation of a modern long-range battery-electric milk truck, rather than as an exact representation of a particular vehicle.

Table 2.1. Main vehicle parameters used in the energy model.

Parameter	Symbol	Value	Unit	Source / note
Gross vehicle mass (fully loaded)	m	55 000	kg	Representative for Swedish milk collection combinations; based on haulier input / literature
Drag coefficient × frontal area	$C_d A$	6.7	m²	Generic value for streamlined heavy-duty tractor + high trailer (literature / reports)
Rolling resistance coefficient	c_{rr}	0.006	–	Typical value for fully loaded trucks on paved roads (literature)
Driveline efficiency (cruise)	η_{drv}	0.92	–	Assumed average battery–motor–driveline efficiency during near-constant-speed operation
Acceleration efficiency	η_{acc}	0.92	–	Assumed equal to η_{drv}; used for kinetic energy changes
Uphill (grade) efficiency	η_h	0.92	–	Assumed equal to η_{drv}; used for potential energy against gravity
Regenerative braking efficiency	n_{regen}	0.70	–	Assumed overall efficiency for energy recovery (machine + inverter + battery)
Nominal battery capacity	$E_{\text{batt,nom}}$	780(example)	kWh	In range of Volvo long-range BEV (≈700–800 kWh); based on manufacturer info + assumptions
Usable SoC – minimum	SoC_{min}	10	% of nominal	Assumed operational lower limit to protect battery lifetime
Usable SoC – maximum	SoC_{max}	90	% of nominal	Assumed operational upper limit to protect battery lifetime
Auxiliary power (base case)	P_{aux}	10	kW	Base case 10 kw for auxiliaries
Gravitational acceleration	g	9.81	m/s²	Physical constant
Air density	ρ	1.225	kg/m³	Standard sea-level value; assumed constant

The main vehicle parameters used in the energy model are summarised in Table 2.1. These values are based on a combination of publicly available data for a long-range Volvo electric truck [5] and generic literature values for heavy-duty vehicles [3,4].”

2.3 Energy model

The energy model estimates the traction and braking energy required for a battery-electric milk truck along the reconstructed route. The route is divided into short segments, and for each segment the model calculates contributions from rolling resistance, aerodynamic drag, road gradient, changes in kinetic energy and auxiliary loads. These are then converted from wheel energy to battery energy using the efficiencies in Section 2.2 [3,4].

2.3.1 Overview and notation

The route is represented as an ordered sequence of points with longitude, latitude, elevation and posted speed limit:

$$(\mathrm{lon}_i, \mathrm{lat}_i, H_i, v_{\max,i}), i = 1, \ldots, N$$

From these points, the model constructs segment-wise quantities for $k = 1, \ldots, N-1$:

- horizontal segment length s_k[m],
- elevation difference $\Delta H_k = H_{k+1} - H_k$[m],
- initial and final speeds $v_{1,k}$and $v_{2,k}$[m/s], based on posted speed limits,
- approximate segment time Δt_k[s].

For each segment k, the battery energy is written as:

$$E_{\mathrm{bat},k} = E_{\mathrm{rull},k} + E_{\mathrm{aero},k} + E_{\mathrm{hojd},k} + E_{\mathrm{kin},k} + E_{\mathrm{aux},k} \quad (2.1)$$

where:

- $E_{\mathrm{rull},k}$is energy for rolling resistance,
- $E_{\mathrm{aero},k}$is energy for aerodynamic drag,
- $E_{\mathrm{hojd},k}$is net potential energy for climbing/descending (including regeneration),
- $E_{\mathrm{kin},k}$is net kinetic energy for acceleration/deceleration (including regeneration),
- $E_{\mathrm{aux},k}$is auxiliary energy (cab heating, electronics, etc.).

The corresponding **state of charge (SoC)** is updated cumulatively as

$$\mathrm{SoC}_{k+1} = \mathrm{SoC}_k - \frac{E_{\mathrm{bat},k}}{E_{\mathrm{batt,usable}}} \quad (2.2)$$

where $E_{\mathrm{batt,usable}}$is the usable battery capacity defined by the SoC window in Table 1.
A list of the main symbols used in this section is provided in Table 1.

2.3.2 Route discretisation

Geographical coordinates are converted to local Cartesian coordinates using a simple planar projection around the first route point:

$$x_i = R(\lambda_i - \lambda_0)\cos(\varphi_0), y_i = R(\varphi_i - \varphi_0)$$

where $R$is the Earth radius, $\lambda_i$and $\varphi_i$are longitude and latitude in radians, and $\lambda_0, \varphi_0$are the longitude and latitude of the first point.
The horizontal distance of segment $k$is then:

$$s_k = \sqrt{(x_{k+1} - x_k)^2 + (y_{k+1} - y_k)^2} \quad (2.3)$$

and the elevation difference is:

$$\Delta H_k = H_{k+1} - H_k.$$

Vehicle speeds are approximated from the posted speed limits:

$$v_{1,k} = \frac{v_{\max,k}}{3.6}, v_{2,k} = \frac{v_{\max,k+1}}{3.6}$$

with the segment time estimated as

$$\Delta t_k = \frac{s_k}{\max(v_{2,k}, 0.1)}$$

to avoid division by very small speeds. In the base case, wind speed is set to zero, so the relative air speed equals the vehicle speed.

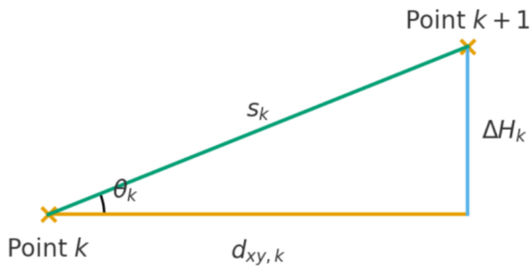

Figure C. Geometry of one route segment between two consecutive points. The horizontal distance d_{xy}, elevation difference $H = \Delta H$and segment length $s$are used to compute road gradient and potential energy changes in the energy model.

2.3.3 Rolling resistance

Rolling resistance is modelled as a constant force proportional to the normal force on the tyres:

$$F_{\text{rull},k} = c_{rr}\, m_k\, g$$

where $c_{rr}$is the rolling resistance coefficient, $m_k$is the vehicle mass in segment k(from the loading model), and $g$is gravitational acceleration.
The corresponding battery energy is

$$E_{\text{rull},k} = \frac{F_{\text{rull},k}\, s_k}{\eta_{\text{drv}}} = \frac{c_{rr}\, m_k\, g\, s_k}{\eta_{\text{drv}}} \quad (2.4)$$

where $\eta_{\text{drv}}$is the average driveline efficiency from battery to wheels during near-constant-speed operation.

2.3.4 Aerodynamic drag

Aerodynamic drag is calculated assuming a constant relative air speed in each segment:

$$F_{\text{aero},k} = \frac{1}{2}\, \rho\, C_d A\, v_{\text{rel},k}^2 \quad (2.5)$$

with

$$v_{\text{rel},k} = \max(v_{2,k} - v_{\text{wind}}, 0)$$

where ρ is air density, $C_d A$ is the product of drag coefficient and frontal area, and v_{wind} is the headwind (zero in the base case).
The corresponding battery energy is:

$$E_{\text{aero},k} = \frac{F_{\text{aero},k}\, s_k}{\eta_{\text{drv}}} = \frac{1}{2}\, \frac{\rho\, C_d A}{\eta_{\text{drv}}}\, v_{\text{rel},k}^2\, s_k. \quad (2.6)$$

2.3.5 Grade and potential energy

Changes in elevation give rise to potential energy changes:

$$\Delta E_{\text{pot},k} = m_k\, g\, \Delta H_k. \quad (2.7)$$

Uphill segments ($\Delta H_k > 0$) require additional battery energy:

$$E_{\text{hojd},k}^{\text{up}} = \frac{m_k\, g\, \Delta H_k}{\eta_h} (\Delta H_k > 0)$$

where $\eta_h$is the effective efficiency for converting battery energy into potential energy.
Downhill segments ($\Delta H_k < 0$) allow regenerative braking. A fraction $n_{\text{regen}}$of the released potential energy is assumed to be recovered to the battery:

$$E_{\text{hojd},k}^{\text{down}} = n_{\text{regen}}\, m_k\, g\, \Delta H_k (\Delta H_k < 0)$$

which is negative because $\Delta H_k < 0$.
The total height-related battery energy for segment k is

$$E_{\text{hojd},k} = \begin{cases} \frac{m_k g \Delta H_k}{\eta_h}, & \Delta H_k > 0 \\ n_{\text{regen}} m_k g \Delta H_k, & \Delta H_k < 0 \\ 0, & \Delta H_k = 0. \end{cases} \quad (2.8)$$

2.3.6 Kinetic energy and regenerative braking

Changes in speed between the start and end of a segment are treated via the kinetic energy:

$$\Delta E_{\text{kin},k} = \frac{1}{2} m_k (v_{2,k}^2 - v_{1,k}^2).$$

For acceleration ($v_{2,k} > v_{1,k}$), additional battery energy is required:

$$E_{\text{kin},k}^{\text{acc}} = \frac{1}{2} \frac{m_k (v_{2,k}^2 - v_{1,k}^2)}{\eta_{\text{acc}}} (v_{2,k} > v_{1,k})$$

where $\eta_{\text{acc}}$is the effective efficiency during acceleration.
For deceleration ($v_{2,k} < v_{1,k}$), regenerative braking can recover part of the kinetic energy:

$$E_{\text{kin},k}^{\text{dec}} = -n_{\text{regen}} \frac{1}{2} m_k (v_{1,k}^2 - v_{2,k}^2)(v_{2,k} < v_{1,k})$$

which is negative because energy is returned to the battery.
Combining these cases:

$$E_{\text{kin},k} = \begin{cases} \frac{1}{2} \frac{m_k (v_{2,k}^2 - v_{1,k}^2)}{\eta_{\text{acc}}}, & v_{2,k} > v_{1,k} \\ -\frac{1}{2} n_{\text{regen}} m_k (v_{1,k}^2 - v_{2,k}^2), & v_{2,k} < v_{1,k} \\ 0, & v_{2,k} = v_{1,k}. \end{cases} \quad (2.9)$$

2.3.7 Auxiliary loads

Auxiliary energy use is represented by a constant auxiliary power P_{aux}acting over the segment time:

$$E_{\text{aux},k} = P_{\text{aux}} \Delta t_k. \quad (2.10)$$

In the base case, $P_{\text{aux}}$is set to zero or a small value to focus on traction energy. Sensitivity analyses can be used to explore the impact of higher auxiliary loads.

2.3.8 Total battery energy and SoC along the route

The total battery energy for segment $k$is finally:

$$E_{\text{bat},k} = E_{\text{rull},k} + E_{\text{aero},k} + E_{\text{hojd},k} + E_{\text{kin},k} + E_{\text{aux},k}.$$

Summing over all segments gives the total battery energy for the route:

$$E_{\text{bat,tot}} = \sum_{k=1}^{N-1} E_{\text{bat},k}. \quad (2.11)$$

The SoC is updated cumulatively along the route as described in Section 2.3.1. If at any point the SoC falls below the minimum allowable SoC, the route cannot be completed without intermediate charging for the chosen vehicle configuration and assumptions. In later sections, this SoC trajectory is used together with the charging model to evaluate the feasibility of the studied milk collection route and to identify where fast charging may be required.

2.3.9 Vehicle mass and load model

The vehicle mass m_k in segment k consists of the empty truck–trailer mass plus the current milk load. Since energy demand is sensitive to vehicle mass, an explicit load model was developed to estimate how much milk is on board after each farm stop along the route.
The starting point is an approximation of the available milk volume at each farm, based on:

- the number of lactating cows at the farm,
- an assumed average milk production of 30 L/cow/day,
- a collection interval of every second day (industry practice),
- and an assumed constant milk density.

The number of lactating cows per farm $N_{\text{cows},f}$ was collected from farm websites and local newspaper articles where available. For each farm f, the theoretical milk volume available at collection is approximated as:

$$V_{\text{milk},f}^{\text{theoretical}} = N_{\text{cows},f} \cdot q_{\text{milk}} \cdot T_{\text{coll}} \quad (2.12)$$

where $q_{\text{milk}} = 30$ L/cow/day is the assumed average daily milk yield and $T_{\text{coll}} = 2$ days is the assumed collection interval. Milk density is assumed to be approximately $\rho_{\text{milk}} \approx 1.0$ kg/L, so the corresponding mass is:

$$m_{\text{milk},f}^{\text{theoretical}} = \rho_{\text{milk}} \, V_{\text{milk},f}^{\text{theoretical}}. \quad (2.13)$$

However, the route data do not directly provide the pumped volume per stop, only the **total stop time** at each farm. To relate stop time to loaded volume, a simple pumping model was introduced based on typical tank and pump specifications for Swedish milk trucks. Tank capacity was assumed to be 38 000–40 000 L, and pump capacity in the range 800–950 L/min. For the calculations, a mid-range pump capacity of

$$r_{\text{pump}} = 875 \text{ L/min}$$

was adopted.
Using a small set of farms where both the number of lactating cows and stop time were known, the theoretical pumping time:

$$t_{\text{pump},f}^{\text{theoretical}} = \frac{V_{\text{milk},f}^{\text{theoretical}}}{r_{\text{pump}}} \quad (2.14)$$

was compared with the observed stop time $t_{\text{stop},f}$. The difference was interpreted as **setup and other non-pumping activities** (positioning the truck, connecting hoses, hygiene routines, disconnecting and paperwork). From this comparison, an average fraction of the stop time spent on setup was estimated as approximately 33% meaning that on average about 67% of the stop time is available for actual pumping.

For each farm stop f along the route, the effective pumping time is therefore approximated as

$$t^{\mathrm{eff}}_{\mathrm{pump},f} = (1 - \alpha_{\mathrm{setup}})\, t_{\mathrm{stop},f} \quad (2.15)$$

with $\alpha_{\mathrm{setup}} \approx 0.33$ denoting the setup fraction. The corresponding pumped volume is:

$$V^{\mathrm{eff}}_{\mathrm{milk},f} = r_{\mathrm{pump}}\, t^{\mathrm{eff}}_{\mathrm{pump},f}, \quad (2.16)$$

and the loaded mass

$$\Delta m_{\mathrm{milk},f} = \rho_{\mathrm{milk}}\, V^{\mathrm{eff}}_{\mathrm{milk},f}. \quad (2.17)$$

The cumulative milk mass on board after farm f is then:

$$m^{\mathrm{onboard}}_{\mathrm{milk},f} = \sum_{j \in \mathcal{F}_f} \Delta m_{\mathrm{milk},j} \quad (2.18)$$

where $\mathcal{F}_f$ is the set of farms visited up to and including f. The total vehicle mass used in segment k is:

$$m_k = m_{\mathrm{empty}} + m^{\mathrm{onboard}}_{\mathrm{milk}}(k), \quad (2.19)$$

where m_{empty} is the assumed empty mass of the truck–trailer and $m^{\mathrm{onboard}}_{\mathrm{milk}}(k)$ is the current milk mass interpolated between farm stops.
To validate the plausibility of this loading model, two complete routes were analysed by summing the estimated pumped volume over all farm stops and comparing it with the nominal tank capacity. The resulting total volumes, on the order of 38–41 m³, fall within or very close to the assumed tank capacity range (38–40 m³) and match operational descriptions that trucks “often arrive full at the dairy”. Sensitivity checks with pump capacities between 800 and 950 L/min and the same setup fraction showed that the total volume remains within a realistic range, indicating that the model is sufficiently accurate for the purpose of simulating mass distribution and energy demand along the route.

The approach does not capture short-term variations in milk yield, herd size changes or detailed on-farm storage practices, but it provides a transparent and operationally grounded estimate of the vehicle mass profile along the route, which is sufficient for the route-level energy and charging analysis in this thesis.

2.4 Charging model

The charging model describes how the battery state of charge (SoC) evolves during charging events along the route. It is used to determine whether the studied milk collection route can be completed:

- with depot and farm charging only, or
- with one or more intermediate DC fast charging stops,

given the assumed vehicle configuration and charging technology.

The model combines:

- a simplified **DC fast charging curve**, relating battery SoC to charging power, and
- a set of **candidate charging locations and operational constraints** along the route.

Charging is only allowed at predefined locations where the truck already stops for operational reasons (e.g. depot, dairy or planned breaks). At such locations, the model can add a charging event, increasing the battery SoC over a charging time Δt^{ch} consistent with the assumed DC charging curve.

The SoC evolution along the route is therefore:

- discharge during driving segments according to the energy model in Section 2.3, and
- discrete charging events at selected stops where SoC is increased.

2.4.1 DC fast charging curve

High-power DC charging of large traction batteries typically follows a characteristic pattern:

1. **Constant-power phase** at or near the maximum charger power, up to a certain SoC, and
2. **Tapering phase**, where charging power is gradually reduced as SoC approaches the upper limit, to protect the battery and stay within voltage/current limits.

To capture this behaviour without modelling electrochemistry in detail, a simplified piecewise charging power curve is assumed as a function of SoC:

- constant maximum power up to a taper threshold SoC,
- linearly decreasing power between the taper threshold and the maximum operational SoC.

Let:

- $P_{\text{DC,max}}$be the maximum DC charging power [kW],
- $\text{SoC}_{\text{taper}}$be the SoC where tapering begins (e.g. 60–70 %),
- SoC_{max}be the maximum operational SoC (e.g. 90 %),
- SoCbe the instantaneous state of charge (fraction of nominal capacity).

The idealised DC charging power is then defined as:

$$P_{\text{DC}}(\text{SoC}) = \begin{cases} P_{\text{DC,max}}, & \text{SoC} \leq \text{SoC}_{\text{taper}} \\ P_{\text{DC,max}} \dfrac{\text{SoC}_{\text{max}} - \text{SoC}}{\text{SoC}_{\text{max}} - \text{SoC}_{\text{taper}}}, & \text{SoC}_{\text{taper}} < \text{SoC} < \text{SoC}_{\text{max}} \\ 0, & \text{SoC} \geq \text{SoC}_{\text{max}}. \end{cases} \quad (2.20)$$

Battery energy content is related to SoC by:

$$E_{\mathrm{batt}} = \mathrm{SoC} \cdot E_{\mathrm{batt,nom}}, \quad (2.21)$$

where $E_{\mathrm{batt,nom}}$is the nominal battery capacity.
For a charging event starting at time $t_0$with initial SoC SoC_0, the SoC development during charging is obtained by integrating the charging power over time, accounting for charger and battery efficiency. In this thesis, this is implemented numerically in MATLAB using a discrete time step Δt, such that SoC is updated according to:

$$\mathrm{SoC}_{j+1} = \mathrm{SoC}_j + \frac{\eta_{\mathrm{ch}} \, P_{\mathrm{DC}}(\mathrm{SoC}_j) \, \Delta t}{E_{\mathrm{batt,nom}}}, \quad (2.22)$$

where $\eta_{\mathrm{ch}}$is an overall charging efficiency (charger + battery). Charging continues until either:

- a target SoC $\mathrm{SoC}_{\mathrm{target}}$(e.g. 80–90 %) is reached, or
- the available dwell time at the charging location is exhausted.

The main input parameters for the charging model are the maximum DC charging power $P_{\mathrm{DC,max}}$, the taper start SoC $\mathrm{SoC}_{\mathrm{taper}}$, the maximum operational SoC $\mathrm{SoC}_{\mathrm{max}}$, and the charging efficiency η_{ch}. These are chosen to be consistent with publicly available specifications for long-range heavy-duty BEVs and DC fast chargers, with a level of detail appropriate for route-level feasibility analysis [3–5].

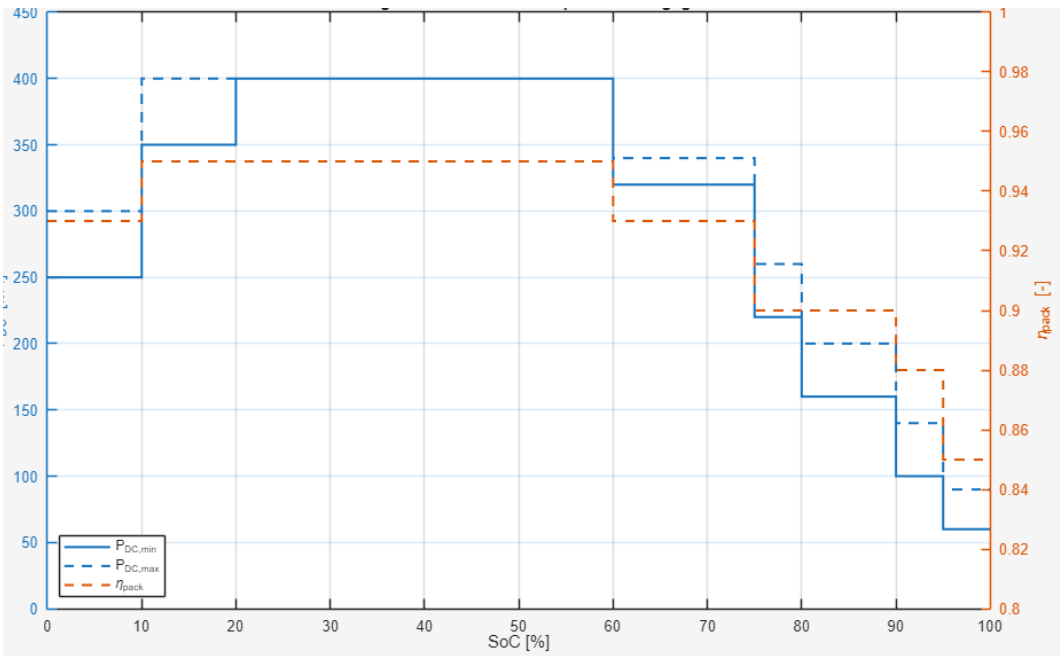

Figure D. *Assumed DC fast charging characteristics as a function of state of charge (SoC). The solid blue line shows the minimum available DC charging power* $P_{DC,min}$*used in the model, while the dashed blue line indicates the nominal maximum charger power* $P_{DC,max}$*. The orange dashed line shows the assumed pack efficiency* η_{pack}*during charging. At low SoC, charging power is limited mainly by the charger (near constant power). As SoC increases, both available power and pack efficiency gradually decrease, representing the tapering behaviour of real high-power charging to protect the battery at high SoC.*

2.4.2 Charging locations and operational constraints

Charging is only permitted at locations where the truck already stops for operational reasons, reflecting the need to integrate charging into existing milk collection routines rather than redesign the route entirely.

In this thesis, the following types of charging locations are considered:

- **Depot or dairy**: start and end points of the route, where overnight or extended charging is possible.
- **Intermediate operational stops**: selected farms or other stopping points where there is sufficient time and practical opportunity to install and use a high-power charger.

The candidate charging locations are identified along the reconstructed route and indexed as $l = 1,2, \dots, L$. For each location l, the model knows:

- the arrival SoC $\mathrm{SoC}_l^{\mathrm{arr}}$,
- the time available for charging $\Delta t_l^{\mathrm{avail}}$(e.g. driven by pumping time and operational constraints),
- the energy required to reach the next critical point on the route.

To determine whether charging is needed at location l, the model estimates the **required battery energy** from l to the next candidate charging location or to the end of the route,

$$E_{\mathrm{req},l} = \sum_{k \in \mathcal{K}_l} E_{\mathrm{bat},k}, \quad (2.23)$$

where $\mathcal{K}_l$denotes the set of driving segments between location l and the next potential charging point. A safety margin E_{margin}can be added to account for uncertainties in the energy model.

The corresponding minimum SoC needed at departure from location l is:

$$\mathrm{SoC}_l^{\mathrm{dep,min}} = \frac{E_{\mathrm{req},l} + E_{\mathrm{margin}}}{E_{\mathrm{batt,usable}}}. \quad (2.24)$$

If the arrival SoC $\mathrm{SoC}_l^{\mathrm{arr}}$is lower than $\mathrm{SoC}_l^{\mathrm{dep,min}}$, the model triggers a charging event at l. Charging is then simulated using the DC charging curve until one of the following conditions is met:

1. SoC reaches a target value $\mathrm{SoC}_{\mathrm{target}}$(e.g. 80–90 %),
2. the minimum required departure SoC $\mathrm{SoC}_l^{\mathrm{dep,min}}$is reached, or
3. the available time $\Delta t_l^{\mathrm{avail}}$is exhausted.

If even with continuous charging during $\Delta t_l^{\mathrm{avail}}$the SoC cannot reach $\mathrm{SoC}_l^{\mathrm{dep,min}}$, the route is classified as **not technically feasible** for the chosen vehicle and charging configuration (under the assumed constraints). This logic is applied sequentially along the route, starting at the depot with an initial SoC within the defined operational window.

Operational constraints included in the model can be summarised as:

- Charging only at predefined locations with existing stops.

- Charging power limited by $P_{\mathrm{DC,max}}$ and the tapering behaviour in Section 2.4.1.
- SoC must remain within the allowable window $[\mathrm{SoC_{min}}, \mathrm{SoC_{max}}]$.
- Charging time at intermediate locations limited by the available dwell time (e.g. milk pumping and setup).

Within these constraints, the charging model provides estimates of:

- total energy charged at each location,
- charging times, and
- peak power requirements at each candidate charging site.

These outputs are later used to discuss the technical feasibility of the studied routes and to provide order-of-magnitude indications of the required charging infrastructure and local grid capacity.

2.4.3 Charging power assumptions and location classes

In practice, the technical and economic feasibility of installing very high-power DC chargers differs strongly between locations. It is much more realistic to assume high-power charging at depots and dairies than at small, remote farms. To reflect this, the analysis distinguishes between two classes of potential charging locations:

- **Class 1 – high-power candidates:**
  Depot and dairy sites, where trucks already park for longer periods and where there is at least a plausible possibility to install high-power DC chargers and reinforce the local grid connection if needed. At these locations, the charging model allows a maximum DC charging power of

$$P_{\mathrm{DC,max}}^{(1)} = 400\ \mathrm{kW},$$

consistent with the upper range of current and announced heavy-duty CCS/“megawatt-class” chargers for trucks. The full DC charging curve in Section 2.4.1 is parameterised using this value.

- **Class 2 – limited-feasibility locations:**
  Intermediate farm stops and other rural locations along the route, where space, grid capacity and practical constraints make installation of very high-power chargers unlikely in the near term. In the **base case**, no DC fast charging is allowed at these locations; they are treated as operational stops only (loading milk, short breaks). In an **exploratory scenario**, a reduced maximum DC power

$$P_{\mathrm{DC,max}}^{(2)} = 150\ \mathrm{kW}$$

is considered to represent the possibility of installing smaller DC chargers or using shared local infrastructure.

In both cases, charging power is further limited by the tapering behaviour of the DC charging curve in Figure D and equation (2.22). The SoC must remain within the operational window

$[\mathrm{SoC}_{\mathrm{min}}, \mathrm{SoC}_{\mathrm{max}}]$, and charging at Class 2 locations is still constrained by the available dwell time determined by pumping and other activities.

The results in Chapter 3 are therefore presented and discussed separately for:

- a **base case** with high-power DC charging only at Class 1 locations (depot/dairy), and
- an **alternative scenario** where reduced-power DC charging is also allowed at selected Class 2 locations.

This classification is later revisited in the Discussion (Chapter 4), where the practical feasibility of installing high-power chargers at dairies and farms is considered in more detail.

3. RESULTS

The results in Tables 3.1–3.3 are reported per stop along the route. In each table, **“Stop 1” denotes the first stop after departure** from the depot or dairy (the departure point itself is not numbered, but is implicitly “Stop 0”). The column “Energy use between stops” shows the modelled battery energy consumption between the previous point and the current stop. For example, in Table 3.1 the value 101.96 kWh at Stop 1 corresponds to the energy used between the departure point and Stop 1, while 157.72 kWh at Stop 2 corresponds to the energy used between Stop 1 and Stop 2, and so on.

By construction, energy use between stops is written with a negative sign in the tables (e.g. −101.96 kWh), indicating battery discharge. The column “Cumulative energy debt” sums the absolute values of these energy uses from the start of the route, and therefore increases as the truck consumes energy along the route. For example, in Table 3.1 the segment from Stop 3 to the haulier’s yard (Stop 4) consumes 332.20 kWh, and the segment from the yard to the dairy (Stop 5) consumes 430.60 kWh.

In Table 3.2, **Stop 1 represents the first stop after the truck leaves the dairy**, i.e. the start of route type 2. The same conventions for energy use between stops and cumulative energy debt apply.

Table 3.1. Segment-wise energy use and charging requirements for route type 1.

The segment-wise battery energy demand and cumulative “energy debt” between stops for route type 1 are summarised in Table 3.1. For each stop, the table shows:

- the **charging class** (1 = high-power candidate, 2 = limited-feasibility location),
- the **battery energy consumption between stops** [kWh],
- the **accumulated energy debt** from the start of the route [kWh],
- the **dwell time** at the stop [min], and
- whether charging is required (“must charge”) or recommended (“should charge”) at that stop.

Stop	Charging class	Energy use between stops [kWh]	Cumulative energy debt [kWh]	Dwell time [min]	Charging requirement	Comment
1	2	−101.96	101.96	49	–	Farm stop, pumping
2	2	−157.72	259.68	11	–	Farm stop
3	2	−12.42	272.10	6	–	Farm stop
4	1	−332.20	604.30	48	Must charge	Haulier yard stop
5	1	−430.60	1 034.90	45	Should charge	Stop at the dairy

For route type 1, the truck leaves the depot and visits three class-2 farm stops (stops 1–3). The energy demand between these stops is 102–158 kWh per leg, resulting in a cumulative energy debt of about 272 kWh at stop 3. At these locations only class-2 charging (or no fast charging) is assumed, and the available dwell times (6–49 min) are primarily used for pumping and other operational tasks. No DC fast charging is therefore applied at these stops in the base case.

The fourth stop is a **class-1 location** at the haulier's yard. The preceding leg is longer and more energy-intensive, with an additional 332 kWh of battery energy consumption, bringing the cumulative energy debt to about 604 kWh. This is close to or above the assumed usable battery capacity for the truck, and the model therefore flags this stop as **"must charge"**. In other words, the route cannot be completed safely without fast charging at this yard stop.

The final leg from the yard to the dairy (stop 5, also class 1) requires a further ~431 kWh, giving a hypothetical cumulative energy debt of around 1 035 kWh if no charging were performed at the yard. Even if the truck is recharged at stop 4, the model indicates that an additional charging event **"should"** be performed at stop 5 before the truck continues towards the dairy and any subsequent duties. This second charging event provides additional operational flexibility and margin against variations in real-world energy use (e.g. due to weather, traffic or auxiliary loads).

Table 3.2. Segment-wise energy use and charging requirements for route type 2.
Segment-wise results for route type 2 are shown in Table 3.2. Compared to route type 1, this route has more stops and a higher total energy demand, with cumulative energy debt approaching roughly 1.8 MWh by the end of the route.

Stop	Charging class	Energy use between stops [kWh]	Cumulative energy debt [kWh]	Dwell time [min]	Charging requirement	Comment
1	1	−235.62	235.62	23	–	Departure from dairy to yard
2	2	−132.61	368.23	4	–	Farm stop
3	2	−12.05	380.28	10	–	Farm stop
4	2	−65.21	445.49	14	–	Farm stop
5	2	−27.61	473.10	11	–	Farm stop
6	2	−225.40	697.88	20	Must charge	Critical point (class 2 location)
7	2	−80.95	778.83	4	–	–
8	2	−70.69	849.52	18	–	–
9	2	−64.99	914.51	8	–	–
10	2	−68.40	982.91	11	–	–
11	1	−49.03	1 031.94	–	–	Class-1 stop

Stop	Charging class	Energy use between stops [kWh]	Cumulative energy debt [kWh]	Dwell time [min]	Charging requirement	Comment
12	1	−523.77	1 555.71	45	Should charge	Example: haulier depot
13	1	−227.24	1 782.95	24	–	End of route

The route starts at a class-1 location near the dairy, with the first leg consuming about 236 kWh and creating an initial energy debt of 236 kWh. The following four farm stops (stops 2–5, class 2) add smaller segments of 12–133 kWh each, leading to a cumulative energy debt of approximately 473 kWh at stop 5. Under the assumed battery configuration, this is still within the usable capacity window and no charging is required at these early stops.

After stop 5, several longer rural segments follow. By stop 6 the cumulative energy debt has increased to roughly 698 kWh, which exceeds the assumed usable battery capacity. Since stop 6 is a **class-2 location** with limited feasibility for high-power chargers, the model marks this as a **critical point**: without either (i) installing at least a moderate-power DC charger at or before stop 6, or (ii) modifying the route, the truck would not be able to complete this section on a single charge.

Continuing the route, additional farm stops further increase the cumulative energy debt, exceeding 1 MWh before the truck reaches the next class-1 location (e.g. a haulier depot) at stop 11–12. The model indicates that at this depot stop the truck **must** or at least **should** charge, depending on the chosen safety margin, in order to maintain sufficient SoC for the remaining part of the route and to reach the end point at stop 13.

In summary, route type 2 is more demanding than route type 1 and cannot be operated reliably using depot and dairy charging alone. Either additional charging capability is needed at one or more intermediate locations (including at least one currently classified as class 2), or the route must be re-planned into shorter electrically feasible sub-routes.

Table 3.3. Segment-wise energy use and dwell times for route type 3.

Stop	Charging class	Energy use between stops [kWh]	Cumulative energy debt [kWh]	Dwell time [min]	Charging requirement	Comment
1	2	−132.97	132.97	10		Farm stop
2	2	−130.32	263.29	13		Farm stop
3	2	−25.18	288.47	17		Farm stop
4	2	−96.47	384.94	11		Farm stop
5	2	−85.69	470.63	44		Farm stop
6	– (no class)	−116.85	587.48	–		Rest area, no charging
7	2	−14.17	601.65	13		Farm stop

Stop	Charging class	Energy use between stops [kWh]	Cumulative energy debt [kWh]	Dwell time [min]	Charging requirement	Comment
8	– (no class)	−4.32	605.97	–	Must charge	Rest area, no charging
9	1	−209.62	815.59	19		Haulier yard (Class 1)
10	– (no class)	−288.45	1 104.04	–		Rest area, no charging
11	1	−323.90	1 427.94	99		Dairy (Class 1), end of route

For route type 3, the cumulative energy debt reaches approximately 1.43 MWh by the final stop at the dairy, with the largest individual energy demands occurring on the legs leading to the haulier's yard (stop 9) and the dairy (stop 11). This makes these two class-1 locations the primary candidates for high-power charging, while the earlier class-2 farm stops mainly influence the depth of discharge before reaching the yard. In the subsequent charging scenarios, route type 3 is therefore evaluated with a focus on yard and dairy charging, with optional lower-power charging at selected farms.

3.1 SoC evolution and charging with base-case assumptions

In this section, the segment-wise energy results from Tables 3.1–3.3 are combined with the charging model to obtain the state of charge (SoC) evolution along each route when DC charging is allowed at all candidate stops. SoC is constrained to the operational window 10–90 % of nominal battery capacity. Tables 3.4–3.6 summarise the SoC at arrival and departure for each stop, together with the energy delivered from the grid and stored in the battery.

Table 3.4. State of charge and charging at each stop for route type 1 (scenario with charging at all stops)

Stop	*Charging class*	*Energy use previous leg [kWh]*	*Arrival SoC before charging [%]*	*Grid energy delivered at stop [kWh]*	*Net energy stored in battery [kWh]*	*Departure SoC after charging [%]*	*Dwell time [min]*	*Comment*
Start	*–*	*–*	*90*	*–*	*–*	*90*	*–*	*Departure from dairy/depot*
1	*2*	*101.96*	*76.9*	*121.4*	*107.8*	*90 (capped)*	*49*	*Farm stop, pumping*

Stop	**Charging class**	**Energy use previous leg [kWh]**	**Arrival SoC before charging [%]**	**Grid energy delivered at stop [kWh]**	**Net energy stored in battery [kWh]**	**Departure SoC after charging [%]**	**Dwell time [min]**	**Comment**
2	*2*	*157.72*	*69.8*	*27.5*	*25.3*	*73.4*	*11*	*Farm stop*
3	*2*	*12.42*	*71.5*	*15.0*	*13.8*	*73.3*	*6*	*Farm stop*
4	*1*	*332.20*	*30.7*	*305.8*	*285.9*	*71.3*	*48*	*Haulier yard stop (must charge)*
5	*1*	*430.60*	*16.1*	*300.0*	*282.1*	*56.2*	*45*	*Dairy stop (should charge)*

Figure E. Graphical representation of Table 3.4 (Route type 1)

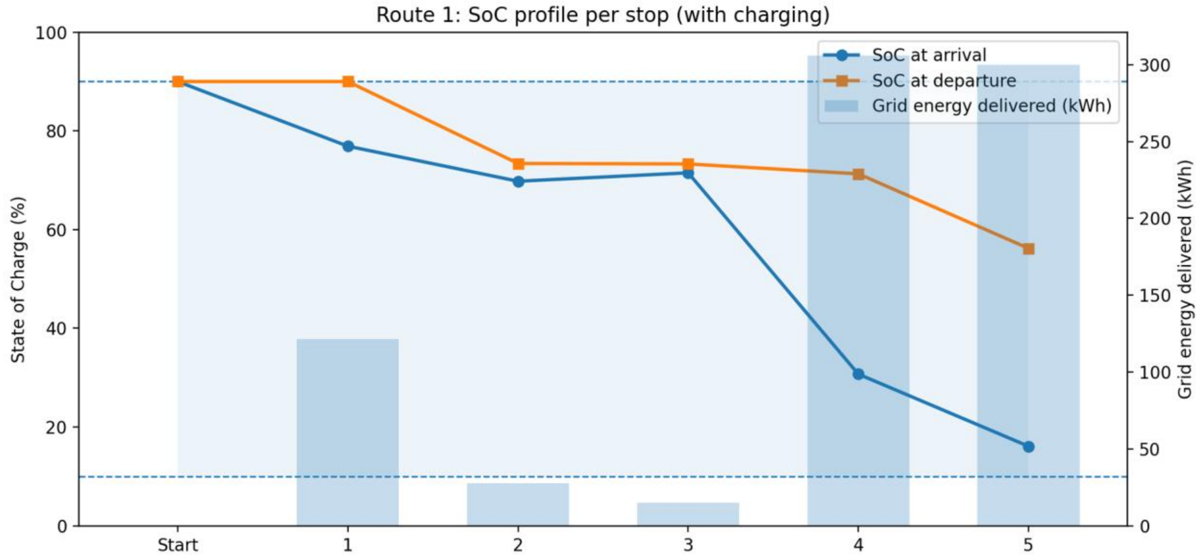

For route type 1, the truck departs the dairy at 90 % SoC and arrives at the first three farm stops (stops 1–3) with SoC values between about 70 and 77 %. The available dwell times at these Class-2 locations allow only modest charging, and the truck leaves stops 2 and 3 with SoC around 73 %.

The fourth stop is the haulier's yard (Class 1). After the long leg from stop 3, the truck arrives at the yard with a low SoC (around 30 %). During the 48-minute stop, approximately 306 kWh is drawn from the grid and about 286 kWh is stored in the battery, increasing the SoC to roughly 71 %. This yard stop is therefore classified as a **"must charge"** location in order to avoid violating the 10 % SoC limit on the final leg.

The last leg to the dairy (stop 5) then reduces the SoC to around 15–20 % on arrival, after which a 45-minute charging session at the dairy increases the SoC to about 56 %. Overall, the route is technically feasible within the 10–90 % SoC window when charging is applied at all stops in Table 3.4.

Table 3.5. State of charge and charging at each stop for route type 2 (scenario with charging at all stops).

Stop	*Charging class*	*Energy use previous leg [kWh]*	*Arrival SoC before charging [%]*	*Grid energy delivered at stop [kWh]*	*Net energy stored in battery [kWh]*	*Departure SoC after charging [%]*	*Dwell time [min]*	*Comment*
Start	*–*	*–*	***56.2***	*–*	*–*	*56.2*	*–*	*Arrival from route type 1 (after dairy charging)*
1	*1*	*235.62*	*26.0*	*153.3*	*144.2*	*46.5*	*23*	*Haulier yard (Class 1)*
2	*2*	*132.61*	*29.5*	*10.0*	*9.4*	*30.8*	*4*	*Farm stop*
3	*2*	*12.05*	*29.3*	*25.0*	*23.5*	*32.6*	*10*	*Farm stop*
4	*2*	*65.21*	*24.2*	*35.0*	*32.9*	*28.9*	*14*	*Farm stop*
5	*2*	*27.61*	*25.4*	*27.5*	*25.9*	*29.1*	*11*	*Farm stop*
6	*2*	*225.40*	***0.2***	*–*	*–*	***0.2***	*20*	*Critical point: SoC below 10 %, route cannot continue*

Figure F. Graphical representation of Table 3.5 (Route type 2)

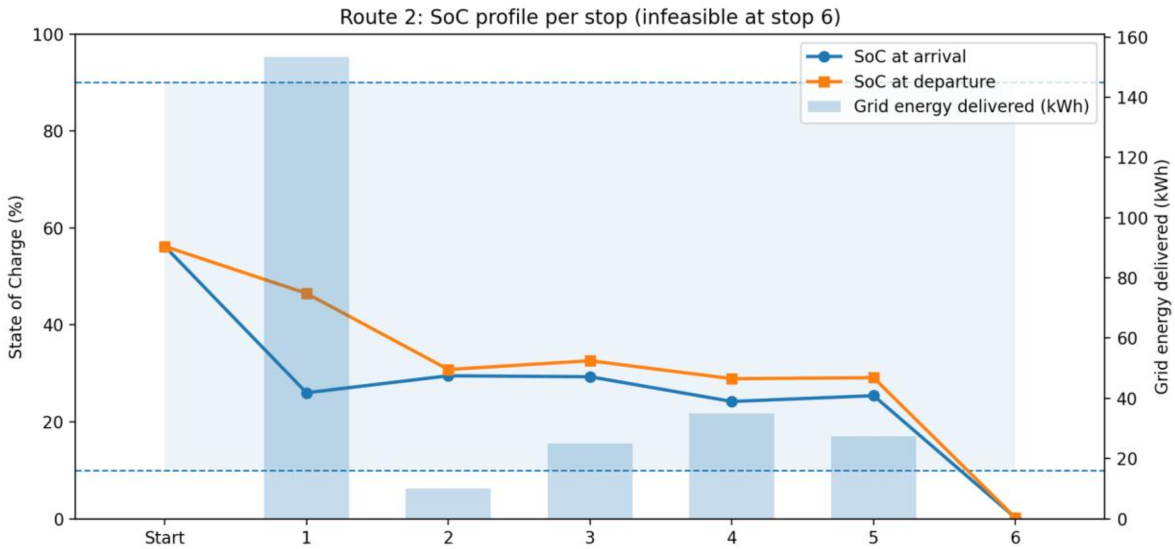

Route type 2 starts from the dairy at 56.2 % SoC, i.e. the SoC at the end of route type 1 after charging at the dairy. The first leg to the haulier's yard (stop 1) reduces the SoC to about 26 %. During the 23-

minute stop at the yard, around 153 kWh is supplied from the grid and 144 kWh is stored in the battery, raising the SoC to 46.5 %.
At the subsequent farm stops (stops 2–5, Class 2), short dwell times and lower charging power lead to only small SoC increases (typically 1–3 percentage points per stop). Despite charging at all these locations, the SoC on arrival at the critical stop 6 is only 0.2 %, i.e. essentially an empty battery. This is well below the minimum allowed SoC of 10 %.
Consequently, even when DC charging is applied at all available stops 1–5 with the current dwell times, route type 2 cannot be completed within the 10–90 % SoC window. Additional charging time or power at one or more stops, or a redesign of the route, would be required to make this route technically feasible.

Table 3.6. State of charge and charging at each stop for route type 3 (scenario with charging at all stops).

Stop	***Charging class***	***Energy use previous leg [kWh]***	***Arrival SoC before charging [%]***	***Grid energy delivered at stop [kWh]***	***Net energy stored in battery [kWh]***	***Departure SoC after charging [%]***	***Dwell time [min]***	***Comment***
Start	*–*	*–*	*90.0*	*–*	*–*	*90.0*	*–*	*Departure from dairy*
1	*2*	*132.97*	*72.9*	*25.0*	*22.8*	*76.1*	*10*	*Farm stop*
2	*2*	*130.32*	*59.4*	*32.5*	*30.0*	*63.7*	*13*	*Farm stop*
3	*2*	*25.18*	*60.5*	*42.5*	*39.1*	*66.1*	*17*	*Farm stop*
4	*2*	*96.47*	*53.8*	*27.5*	*25.9*	*57.5*	*11*	*Farm stop*
5	*2*	*85.69*	*46.5*	*110.0*	*103.3*	*61.2*	*44*	*Farm stop (long dwell)*
6	*– (no class)*	*116.85*	*46.2*	*–*	*–*	*46.2*	*–*	*Rest area, no charging*
7	*2*	*14.17*	*44.4*	*32.5*	*30.6*	*48.8*	*13*	*Farm stop*
8	*– (no class)*	*4.32*	*48.2*	*–*	*–*	*48.2*	*–*	*Rest area, no charging*
9	*1*	*209.62*	*21.4*	*126.7*	*119.1*	*38.4*	*19*	*Haulier yard (Class 1)*
10	*– (no class)*	*288.45*	***1.4***	*–*	*–*	***1.4***	*–*	*Rest area, no charging –* ***SoC < 10% (critical)***

Figure G. Graphical representation of Table 3.6 (Route type 3).

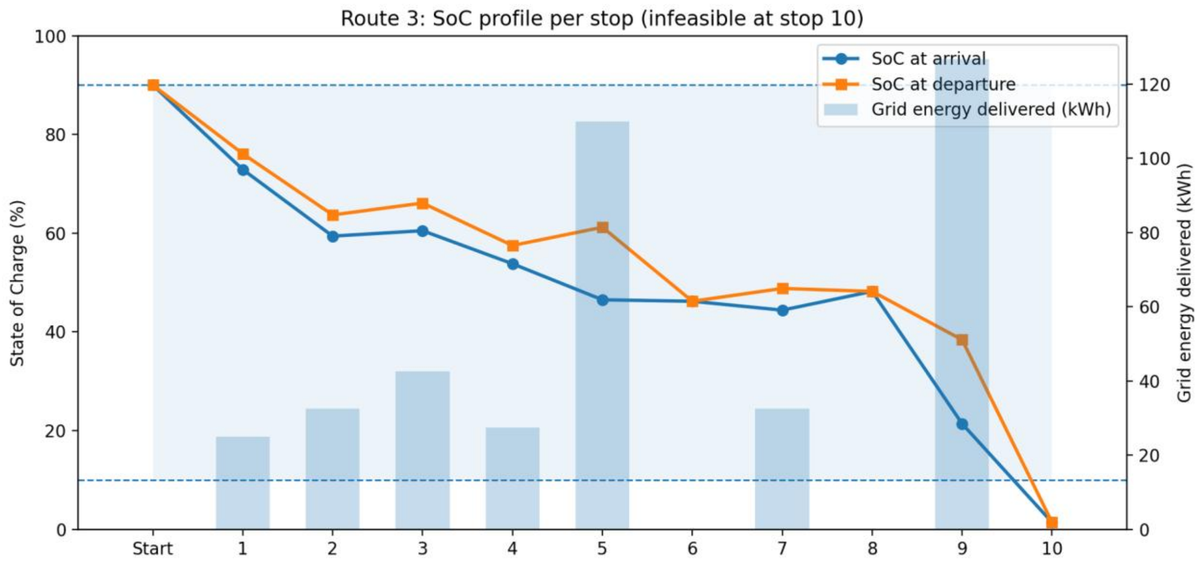

For route type 3, the truck departs the dairy at 90 % SoC. At the first five farm stops (stops 1–5, Class 2), the SoC fluctuates between about 46 and 76 %, with the longer 44-minute stop 5 allowing a larger charge of approximately 110 kWh and a departure SoC of 61.2 %. The subsequent rest area at stop 6 has no charging, and the SoC after stops 6 and 7 remains in the range 44–49 %.

After the short rest at stop 8 (no charging), the truck reaches the haulier's yard at stop 9 with a SoC of about 21 %. A 19-minute charging session at this Class-1 location supplies around 127 kWh from the grid and stores 119 kWh in the battery, raising the SoC to 38.4 %. However, the following long leg to stop 10 consumes 288.45 kWh, leaving the truck with only 1.4 % SoC on arrival at this rest area, again below the 10 % minimum.

As shown in Table 3.6, even with charging at all farm stops and at the haulier yard, **route type 3 cannot be completed without violating the SoC constraint**: the state of charge at stop 10 falls below 2 %, and the final leg to the dairy (stop 11) is not reachable in this scenario.

4.DISCUSSION

4.1 Synthesis of main findings

The modelling results show clear differences in electrification feasibility between the three studied milk collection routes. Route type 1, which has a moderate total energy demand and a limited number of long, high-speed segments, can be operated within the assumed 10–90 % SoC window when DC charging is applied at all candidate stops. With charging at the three farm stops, the haulier's yard and the dairy, the truck completes the route and arrives back at the dairy with a SoC of around 15–20 %, after which a final charging session raises the SoC to about 56 %. In other words, route type 1 appears technically feasible for a long-range battery-electric truck under the assumed conditions.

In contrast, route types 2 and 3 prove substantially more demanding. For route type 2, even when DC charging is allowed at every stop from 1 to 5 (yard and farms), the state of charge at the critical stop 6 falls to about 0.2 %, far below the minimum allowed SoC of 10 %. The route cannot be completed without violating the SoC constraint, regardless of how the available dwell times are used at earlier stops. A similar pattern is observed for route type 3: despite multiple charging events at farms and at the haulier yard, the SoC on arrival at stop 10 is only about 1.4 %, and the final leg to the dairy (stop 11) is not reachable within the 10–90 % SoC window.

Taken together, these results suggest that **some milk collection routes can be electrified with today's battery sizes and realistic charging powers**, while other routes are so energy-demanding that they remain infeasible without more fundamental changes. The decisive factors are the total energy requirement, the distribution of that requirement over the route (long high-speed segments vs many short legs) and the availability of sufficiently long dwell times at locations where high-power charging is realistic[3,4].

The analysis also indicates which parts of the energy demand dominate. For all routes, rolling resistance and aerodynamic drag constitute a large share of the total energy consumption, consistent with the high gross vehicle mass and the mix of rural and highway driving. Elevation changes and kinetic energy (acceleration/braking) make a noticeable contribution, but are partly mitigated by regenerative braking. Auxiliary loads are small in the base case, but could become more important in winter conditions or for refrigerated operation. This component breakdown is important when interpreting the effects of different mitigation strategies, such as reducing speed, improving aerodynamics or changing route planning.

4.2 Methodological reflections and limitations

The results should be interpreted in light of several methodological choices. First, the energy model is based on reconstructed routes rather than directly measured trajectories. Event-based logs from the haulier were translated into start/stop coordinates and routed through GPX Studio to obtain a continuous polyline, with elevation and speed limit data attached from SRTM and OpenStreetMap[6–8]. This yields a realistic but not exact representation of the driven routes. Small deviations in alignment or gradient may lead to over- or underestimates

of energy use on individual segments, although the overall distance and topography remain plausible.
Second, the speed along each segment is approximated by the posted speed limit. In reality, trucks often travel slightly below the limit, especially on smaller roads, and may be constrained by traffic, curves, or farm access conditions. Using speed limits therefore tends to **overestimate aerodynamic losses**, particularly on roads where the actual speed is consistently below the limit. On the other hand, the model does not include any explicit penalties for stop-and-go traffic, queuing or manoeuvring at farms, which could increase kinetic energy losses. The net effect is uncertain, but the simplification should be kept in mind when interpreting numerical SoC margins.
Third, the load model is approximate. The number of lactating cows at each farm was inferred from websites and media sources, and combined with a standard milk yield and a fixed collection interval to estimate the available milk volume. Pumping times were not recorded in the route logs and were reconstructed using an assumed pump capacity and a typical setup fraction of the stop time. This produces a physically reasonable mass profile along the route and ensures that total collected volumes are consistent with tank capacities, but it does not capture farm-to-farm variation in production, herd changes or on-farm storage practices. Since vehicle mass directly influences rolling and grade energy, this is a source of uncertainty.
Fourth, battery and charging parameters are partly based on indicative manufacturer information for a long-range Volvo electric truck and partly on generic literature values. The nominal battery capacity of 780 kWh and the 10–90 % operational SoC window are plausible but not unique choices. A different truck, a slightly larger pack or a different SoC window would shift the feasibility thresholds. Likewise, the assumed DC charging powers (400 kW for Class 1 locations and 150 kW for Class 2 farms) represent the upper end of what is considered realistic today; lower power levels would make the infeasibility of routes 2 and 3 even more pronounced.
Finally, the charging strategy itself is simplified. In the base-case scenarios, the truck charges “as much as possible” at each stop within the given dwell time and power limit, rather than following a fully optimised charging schedule. This heuristic is reasonable for exploring feasibility, but it does not guarantee that the absolute minimum number of chargers or minimum total charging time has been found. A full optimisation-based charger siting and sizing study would be needed to answer such questions. Nonetheless, the fact that route types 2 and 3 remain infeasible even under a generous “charge everywhere” assumption is a robust indication of their difficulty.

4.3 Implications for electrification of milk collection

From an operational perspective, the results illustrate that the electrification potential is **route-specific[3,4]**. Route 1 can be electrified using a single long-range BEV, provided that high-power charging is available at the haulier’s yard and at the dairy, and that lower-power charging is used opportunistically at farms. For such routes, the main barriers are likely to be investment cost and practical integration of charging into daily routines, rather than fundamental range limitations.

For route 2 and 3, however, the analysis shows that electrification is not simply a matter of adding one or two chargers. Even when DC charging is enabled at all farms and at the yard, with the current dwell times and charging powers, the battery is effectively depleted before reaching the next critical stop. For route 2, this happens at stop 6; for route 3, it occurs at stop 10. Overcoming this would require substantial additional energy to be supplied somewhere along the route. In practice, this might involve:

- significantly higher peak power at depot or dairy (e.g. >400 kW),
- longer dwell times at key farms, or
- the introduction of additional intermediate charging hubs.

Each of these options has drawbacks. Installing and using 400–1000 kW chargers at dairies or yards poses challenges for the local grid and requires substantial investment. For dispersed farms, even 150 kW can imply step changes in local grid capacity, new transformers and potentially long lead times for network reinforcement. Extending dwell times at farms increases driver and vehicle time and may conflict with tight collection schedules. Interviews with the haulier also suggested that the cost per kilometre for current heavy-duty electric trucks is already significantly higher than for conventional diesel operation, even without considering grid reinforcements and potential downtime for charging[10]. Under such conditions, further increasing dwell times or adding very high-power charging could be difficult to justify.

It should also be noted that the assumed DC power level of 150 kW at farms is already optimistic for many rural locations. Typical farm connections are dimensioned for on-farm loads (milking equipment, cooling, ventilation, etc.) rather than for supplying continuous high-power charging to heavy-duty vehicles. Installing 150 kW chargers at farms would in many cases require new transformers and upgraded grid connections. Peak powers substantially above 150 kW at individual farms are therefore likely to be technically and economically challenging, even for larger producers. In this sense, the “charge at all farms with 150 kW” scenario represents a favourable upper-bound case for what might be achievable at Class-2 locations.

These findings suggest that **route redesign and system-level changes may be at least as important as charging technology** for the electrification of long and energy-intensive milk runs. Rather than forcing a single long-range BEV to complete a route that is marginal even with aggressive charging, it may be more effective to:

- split long routes into two shorter BEV-compatible routes,
- deploy an additional vehicle to cover the most distant farms, or
- rearrange farm allocations between routes to keep total energy demand per truck within the usable window.

Such changes would require co-ordination between dairies and hauliers, but the modelling here provides a first indication of where they may be necessary.

A related question is how the **costs and benefits of electrification are distributed between actors**. The main infrastructure investments for charging and potential grid reinforcements would likely fall on the haulier and, in the case of farm-based chargers, on individual farmers. The main climate benefits and potential image gains, however, accrue primarily to the dairy and the wider supply chain. Interviews with the haulier indicated that the cost per kilometre for current electric trucks can already be significantly higher than for diesel trucks, even without counting grid upgrades[10]. This raises questions about which party is expected to finance additional charging infrastructure, and what incentives or support schemes would be needed for hauliers and farmers to invest. A full analysis of these institutional and economic aspects is beyond the scope of this thesis, but the results here suggest that successful electrification of longer milk routes will require not only technical solutions, but also coordinated investment and cost-sharing between dairies, hauliers and farmers.

5. CONCLUSIONS

5.1 Main findings

The technical feasibility of electrifying selected milk collection routes with a battery-electric heavy-duty truck was evaluated using a segment-wise physics-based energy model and a time-constrained DC fast-charging representation. Under the assumed long-range truck configuration and the chosen operational state-of-charge (SoC) window, **one of the three studied routes was found to be technically feasible**, while **two routes were found to be infeasible** within the operational constraints reflected in the route logs.
Overall feasibility was found to be **limited for full electrification** when normal operational conditions were maintained, i.e., when route duration, stop durations and realistic charging opportunities were not substantially altered. The dominant bottleneck was identified as **charging time availability**, which is coupled to the need for **high-power charging infrastructure** at locations where sufficient dwell time exists. Since charging powers at both depot/dairy and farms were treated using **plausible but optimistic assumptions**, feasibility for the more demanding routes was assessed to be weaker in practice, as implementation would likely require grid reinforcement and/or operational changes that may be difficult to justify.

5.2 Conclusions in relation to the research questions

RQ1 – Route energy demand and SoC trajectories

Segment-wise modelling showed that energy demand and SoC trajectories varied substantially between routes. Feasibility could not be inferred from route distance alone, as road gradients, speed limits, auxiliary loads and the increasing payload during collection were found to influence the SoC evolution and the occurrence of critical low-SoC points.

RQ2 – Feasibility when charging during operational stops
When charging was allowed during operational stops and charging power was determined using a literature-based DC charging curve, the energy added during available dwell times was sufficient to maintain feasible operation only for route1. For the infeasible routes, the energy deficit could not be compensated within existing stop durations, even when charging was permitted at all candidate stops. This indicates that the routes are constrained primarily by the combination of required charging energy and limited stop time.

RQ3 – Infrastructure requirements and bottlenecks under optimistic assumptions
Under plausible but optimistic charging assumptions (high-power charging at depot/dairy and limited fast charging at farms), feasibility was found to be strongly constrained by **charging time and charging power**, rather than by battery capacity alone. In practice, widespread fast charging at farms was assessed to be unlikely without grid reinforcement, and even depot/dairy high-power charging may require non-trivial electrical upgrades depending on site conditions. While increased dwell times could improve feasibility, such changes would risk violating operational time windows and could therefore require extensive adaptations (e.g., route redesign, additional vehicles, or intermediate charging hubs).

5.3 Implications

The results indicate that electrification potential for milk collection is route-dependent and that full electrification of more demanding routes is unlikely to be achieved without coordinated investments in charging infrastructure and/or significant operational changes. For routes similar to the infeasible cases, feasible electrification is likely to require measures such as route segmentation into shorter sub-routes, additional vehicles, or strategically placed high-power charging hubs that can provide substantial energy within limited time.

6. RECOMMENDATIONS

Based on the results of this thesis, immediate full electrification of the more energy-demanding milk collection routes is not recommended as a default approach when operations are required to remain within the route duration and stop-time constraints reflected in current route logs. Feasibility was primarily limited by charging time availability, implying a need for high-power charging infrastructure at locations with sufficient dwell time. Since the charging assumptions applied in this study were already optimistic—particularly for farm-based charging—implementation would likely require grid reinforcement and/or operational changes such as longer stops, route redesign or additional vehicles.

7. FUTURE WORK AND FURTHER IMPROVMENTS

Several improvements and extensions of the present work are possible.
First, the energy and load models could be calibrated and validated against measurements from real electric trucks. Access to time-resolved speed, SoC and power data would allow direct comparison between modelled and measured consumption and would reduce uncertainty related to speed profiles, auxiliary loads and regenerative braking. Similarly, improved farm-level data on milk volumes and pumping operations would refine the vehicle mass profile along the route.
Second, the charging analysis could be extended beyond the heuristic “charge at all stops” approach. A natural next step would be to formulate and solve an optimisation problem for charger siting, sizing and scheduling, subject to SoC constraints, dwell times and simple grid capacity limits. This would make it possible to identify the minimum number and power of chargers required to make a given set of routes feasible, and to quantify trade-offs between battery size, number of vehicles and infrastructure investment.
Third, the present study treats grid capacity and electricity prices only implicitly. Incorporating a simplified representation of local grid constraints and time-varying electricity prices would enable a first assessment of the economic feasibility of different charging strategies and locations, and could be linked to the interview findings on cost per kilometre.
Finally, the analysis could be broadened to include more routes and alternative technologies. Additional milk collection routes in other regions could be added to examine how widely the findings generalise. Comparisons with other decarbonisation options, such as HVO, biogas or hydrogen fuel-cell trucks, could also be made to place battery-electric operation in a wider context. Together, these extensions would provide a more comprehensive picture of the role that battery-electric trucks can realistically play in the electrification of milk collection logistics[3,4].

REFERENCES

[1] International Energy Agency (IEA). *Trucks and buses – Analysis*. Paris: IEA; 2025.
[2] European Environment Agency (EEA). *Greenhouse gas emissions from transport in Europe*. Copenhagen: EEA; 2025.
[3] Nykvist B, Olsson O. The feasibility of heavy battery electric trucks. *Joule*. 2021;5(4):901–913.
[4] Link S, Plötz P. Technical feasibility of heavy-duty battery-electric trucks for urban and regional delivery in Germany – A real-world case study. *World Electric Vehicle Journal*. 2022;13(9):161.
[5] Volvo Trucks. Breakthrough: Volvo to launch electric truck with 600 km range. Press release. Gothenburg: Volvo Trucks; 3 Sep 2024. Available from: https://www.volvotrucks.com/en-en/
[6] NASA Jet Propulsion Laboratory (JPL). *Shuttle Radar Topography Mission (SRTM)*. Pasadena (CA): NASA; 2020.
[7] US Geological Survey (USGS). *USGS EROS Archive – Shuttle Radar Topography Mission (SRTM) Void Filled*. Reston (VA): USGS; 2018.
[8] OpenStreetMap contributors. About OpenStreetMap. 2025. Available from: https://www.openstreetmap.org/#map=5/62.99/17.64
[9] GPX Studio. gpx.studio – the online GPX file editor and route planner. 2025. Available from: https://gpx.studio/
[10] Mejeritransporter TJ AB. Interview about electrification of milk collection routes. Interview with transport manager, conducted by Haqvin Wedelsbäck; 10 Aug 2025; Karlstad. (In Swedish).

8.POPULAR SCIENCE SUMMARY

Swedish milk production was already relatively climate-efficient, but the trucks used for collecting milk from farms were almost entirely diesel-powered. Heavy-duty vehicles accounted for a large share of road-traffic emissions, and both Sweden and the EU aimed to reduce these emissions substantially over the coming decades. An important question was therefore whether milk collection could be electrified using battery-electric trucks without jeopardising daily collection schedules and farm operations.

In this thesis, three real milk collection routes operated by a Swedish milk haulier were analysed. The routes started from a dairy and a haulier's depot in central Sweden and included both shorter and longer trips, as well as different road types. The main question was whether a modern long-range battery-electric truck could complete these routes given realistic opportunities for charging during the operational day.

The work was conducted in three main steps. First, the routes were reconstructed using the haulier's trip logs together with digital maps and elevation data. Second, a physics-based energy model was developed to estimate the energy demand along each route segment. The model accounted for vehicle mass, rolling resistance, aerodynamic drag, road gradients and the increasing payload as milk was loaded at successive farm stops. Third, a charging model was applied to track changes in battery state of charge (SoC) during DC fast charging at different stop locations.

Based on interviews with the haulier and publicly available information, a representative long-range battery-electric truck configuration comparable to Volvo's announced long-range electric truck was selected. An installed battery capacity of 780 kWh was assumed, with an operational SoC window of 10–90% to reflect typical battery-use limitations. At the depot and dairy, the availability of high-power charging around 400 kW was assumed, while farms were assumed to provide up to 150 kW at best. This farm-charging assumption was considered optimistic, since many farms would require substantial upgrades to their electrical connection to deliver such power levels.

The results showed that one of the three routes could be electrified under these assumptions. For this route, DC fast charging at the haulier's yard and at the dairy was sufficient, complemented by short charging opportunities at a limited number of farm stops. Battery SoC remained within the allowed operating window and some margin was retained for factors such as cold weather, operational variation or additional stops.

For the other two routes, feasibility was not achieved. These routes were longer, included more hilly and high-speed driving, and offered fewer suitable charging opportunities. Even when charging was permitted at every farm stop and full dwell time was utilised, battery SoC still dropped below the minimum threshold before route completion. For one route, this occurred at a farm stop in the afternoon; for the other, it occurred at a rest area shortly before the final stretch to the dairy. Under the investigated assumptions, these routes could therefore not be operated reliably with a single battery-electric truck.

Making these routes feasible would have required substantially more energy to be supplied during the day, through higher charging power at the depot and dairy, longer charging times at farms, and/or new dedicated charging locations. Each option implied higher costs and practical challenges. Very high-power charging would likely require new transformers and local grid reinforcement. Longer charging stops would reduce productive driving time and risk disrupting existing collection schedules. Interviews also indicated that the perceived cost per kilometre for current electric heavy-duty trucks was already higher than for diesel, even before grid-upgrade costs were considered.

Overall, electrification was indicated to be not only a technical question of trucks and chargers, but also an operational and organisational question involving route design and the sharing of investment responsibilities between dairies, hauliers and farmers. For some routes, battery-electric trucks appeared to be a realistic alternative already under optimistic charging assumptions. For more demanding routes, a combination of shorter routes, additional vehicles, strategically located charging hubs and new forms of cooperation around financing and operation was likely required. The modelling framework developed in this thesis provided a practical first tool for identifying which routes were most suitable for electrification and where the primary bottlenecks were located for the more challenging cases.

APPENDIX A

A.1 MATLAB script for route energy model

```
%% ROUTE ENERGY FROM PASTED POINTS (lon/lat/speed/ele)
% Klistra in dina rader i raw_points nedan så kör det direkt.

%% ---- KONSTANTER (ändra vid behov) ----
m          = 55000;         % kg (GTW)
g          = 9.81;          % m/s^2
rho        = 1.225;         % kg/m^3
CdA        = 6.7;           % m^2
crr        = 0.006;         % -
eta_drv    = 0.92;          % -
eta_h      = 0.92;          % - (uppför)
eta_acc    = 0.92;          % - (acceleration)
n_regen    = 0.70;          % - (broms/regen)
P_aux      = 10000;            % W (0 om okänt)
use_wind_ms = 0;            % m/s, + med-/ - motvind. Sätt 0 om okänt.

%% ---- DATAINMATNING: KLISTRA IN PUNKTER HÄR ----
raw_points = [



% ... KLIPPA-IN HELA LISTAN HÄR (alla rader i samma stil) ...
];

% Alternativ: läs från fil i samma format (kommentera bort raderna ovan)
% raw_points = string(splitlines(fileread('lon_lat_speed_ele_labeled_FILLED_all.txt')));
% raw_points(raw_points=="") = [];

%% ---- PARSING ----
N = numel(raw_points);
lon = nan(N,1); lat = lon; vmax_kmh = lon; ele = lon;

expr = "lon=(?<lon>[-\d\.]+),\s*lat=(?<lat>[-\d\.]+),\s*maxspeed_kmh=(?<v>[-\d\.]+),\s*ele_m=(?<ele>[-\d\.]+)";
for i = 1:N
    t = regexp(raw_points(i), expr, 'names');
    if isempty(t), error('Rad %d följer inte formatet.', i); end
    lon(i)     = str2double(t.lon);
    lat(i)     = str2double(t.lat);
    vmax_kmh(i)= str2double(t.v);
    ele(i)     = str2double(t.ele);
```

```
end

%% ---- LAT/LON → LOKALA METER (plan projektion runt första punkten) ----
R     = 6371000;          % Jordradie ~m
lat0  = deg2rad(lat(1));
lon0  = deg2rad(lon(1));
x = R * (deg2rad(lon) - lon0) .* cos(lat0);
y = R * (deg2rad(lat) - lat0);

%% ---- SEGMENTSTORHETER ----
dx  = diff(x);   dy = diff(y);
dxy = hypot(dx,dy);          % [m]
dH  = diff(ele);             % [m]
v2  = vmax_kmh(2:end) * (1000/3600);   % [m/s] sluthastighet i segment
v1  = vmax_kmh(1:end-1) * (1000/3600); % [m/s] starthastighet i segment

% Relativhastighet mot luft (justera vind):
v_rel = max(v2 - use_wind_ms, 0);  % enkel modell; sätt 0 om det blir negativt

% Approx segmenttid (för E_aux). Utan faktisk tidsstämpel använder vi v2.
dt = dxy ./ max(v2, 0.1);      % [s] skydd mot /0

%% ---- ENERGIER PER SEGMENT ----
% Rullmotstånd
E_rull = (crr * m * g / eta_drv) .* dxy;

% Aerodynamik
E_aero = 0.5 * (rho * CdA / eta_drv) .* (v_rel.^2) .* dxy;

% Hjälpsystem
E_aux  = P_aux .* dt;

% Höjd (uppför: mg*ΔH/eta_h; nedför: ΔH*mg*n_regen)
E_h_up   = (dH > 0) .* (m * g .* dH ./ eta_h);
E_h_down = (dH < 0) .* (m * g .* dH .* n_regen);   % dH<0 → negativt (återvinning)
E_hojd   = E_h_up + E_h_down;

% Kinetik (styckvis)
E_kin = zeros(size(dxy));
accIdx = v2 > v1;
decIdx = v2 < v1;
E_kin(accIdx) = 0.5 * m .* (v2(accIdx).^2 - v1(accIdx).^2) ./ eta_acc;
E_kin(decIdx) = - n_regen * 0.5 * m .* (v1(decIdx).^2 - v2(decIdx).^2);
```

```
% Summa per segment & total
E_seg = E_rull + E_aero + E_aux + E_hojd + E_kin;   % [J]
E_tot_J   = sum(E_seg);
E_tot_kWh = E_tot_J / 3.6e6;

%% ---- UTSKRIFT ----
fprintf('Antal segment: %d\n', numel(dxy));
fprintf('Total batterienergi: %.2f kWh\n', E_tot_kWh);
fprintf(' - Rull:  %.2f kWh\n', sum(E_rull)/3.6e6);
fprintf(' - Aero:  %.2f kWh\n', sum(E_aero)/3.6e6);
fprintf(' - Aux:   %.2f kWh (P_aux=%.0f W)\n', sum(E_aux)/3.6e6, P_aux);
fprintf(' - Höjd:  %.2f kWh (inkl. regen)\n', sum(E_hojd)/3.6e6);
fprintf(' - Kinetik: %.2f kWh (inkl. regen)\n', sum(E_kin)/3.6e6);

%% ---- ENKLA PLOTTAR (valfritt) ----
figure; plot((1:numel(dxy)), E_seg/3.6e6, '.-'); xlabel('Segment'); ylabel('E_{bat,seg} [kWh]'); title('Batterienergi per segment');
figure; plot(x/1000, ele, '.-'); xlabel('x [km]'); ylabel('Höjd [m]'); title('Höjdprofil');
```

A.2 MATLAB script for DC fast charging curve and pack efficiency

```
%% Laddkurva enligt punktlistan (SoC i %)

% SoC-intervallens kanter
soc_edges = [0 10 20 60 75 80 90 95 100];   % [ % ]

% Effektintervall (kW) per SoC-intervall
P_min = [250 350 400 320 220 160 100  60];  % lägre värde
P_max = [300 400 400 340 260 200 140  90];  % högre värde

% Packverkningsgrad per intervall
eta_pack = [0.93 0.95 0.95 0.93 0.90 0.90 0.88 0.85];

% Gör dem "styckvisa konstanta" över hela laddintervallet
P_min_plot  = [P_min  P_min(end)];
P_max_plot  = [P_max  P_max(end)];
eta_plot    = [eta_pack eta_pack(end)];

%% Plot

figure; clf

yyaxis left
```

```
stairs(soc_edges, P_min_plot, 'LineWidth', 1.5); hold on
stairs(soc_edges, P_max_plot, 'LineWidth', 1.5);
ylabel('P_{DC} [kW]')
ylim([0 450])

yyaxis right
stairs(soc_edges, eta_plot, 'LineWidth', 1.5, 'LineStyle', '--');
ylabel('\eta_{pack} [-]')
ylim([0.8 1.0])

grid on
xlabel('SoC [%]')
title('Föreslagen DC-laddkurva och packverkningsgrad')
legend('P_{DC,min}', 'P_{DC,max}', '\eta_{pack}', 'Location', 'southwest')
```

A.3 MATLAB script for SoC after DC fast charging with limited time

```
%% Laddslut-SoC baserad på föreslagen DC-laddkurva och given laddtid


clear; clc;


%% ---- Batteri- och laddarparametrar ----
E_installed_kWh = 780;     % Installerad batterikapacitet [kWh]
f_usable        = 0.90;    % Användbar andel av kapaciteten [-]

soc_start = 21.4;           % Start-SoC [%]

P_AC_avail = 400;          % Max AC-effekt från elnät/laddare [kW]
eta_rect   = 0.99;         % Verkningsgrad likriktare/kablar [-]

% Tillgänglig laddtid
t_avail_min = 19 ;          % Tillgänglig laddtid [min]
t_avail_h   = t_avail_min/60;  % [h]

%% ---- Laddkurva (packbegränsning) ----
% SoC-intervallens kanter [%]
soc_edges = [0 10 20 60 75 80 90 95 100];

% DC-effekt per intervall [kW]
P_DC_min = [250 350 400 320 220 160 100  60];  %#ok<NASGU>  % ej nödvändig men sparas
P_DC_max = [300 400 400 340 260 200 140  90];              % max DC-effekt

% Packverkningsgrad per intervall [-]
```

```
eta_pack = [0.93 0.95 0.95 0.93 0.90 0.90 0.88 0.85];

nSeg = numel(P_DC_max);

%% ---- Beräkning av SoC efter given tid ----
t_seg_h        = zeros(1,nSeg);   % faktisk tid i varje segment [h]
E_batt_seg_kWh = zeros(1,nSeg);   % energi lagrad i batteriet [kWh]
E_grid_seg_kWh = zeros(1,nSeg);   % energi tagen från nätet [kWh]

soc_curr = soc_start;   % aktuell SoC [%]
t_rem_h  = t_avail_h;   % återstående tid [h]

for k = 1:nSeg

   if t_rem_h <= 0
      break;  % ingen tid kvar att ladda
   end

   % SoC-omfång för segment k
   s_lo = soc_edges(k);
   s_hi = soc_edges(k+1);

   % Om vi redan är förbi detta segment, hoppa vidare
   if soc_curr >= s_hi
      continue;
   end

   % Start-SoC inne i detta segment
   s1 = max(s_lo, soc_curr);   % [%]

   % Max SoC-ökning som ryms kvar i detta segment
   delta_s_max = (s_hi - s1)/100;    % [-] (andel av full SoC)

   if delta_s_max <= 0
      continue;
   end

   % Max energi in i batteriet om vi fyller segmentet till s_hi
   E_seg_max_kWh = delta_s_max * f_usable * E_installed_kWh;   % [kWh]

   % Packbegränsad AC-effekt: DC_max / eta_rect
   P_AC_pack_lim = P_DC_max(k) / eta_rect;
```

```
% Faktiskt möjlig AC-effekt i segmentet [kW]
P_AC_k = min(P_AC_avail, P_AC_pack_lim);

% Total verkningsgrad AC -> lagrad energi [-]
eta_tot_k = eta_rect * eta_pack(k);

% Effekt som faktiskt lagras i batteriet [kW_batt]
P_batt_k = P_AC_k * eta_tot_k;   % [kW]

% Tid som krävs för att fylla kvarvarande del av segmentet [h]
t_needed_k = E_seg_max_kWh / P_batt_k;

if t_rem_h >= t_needed_k
    % Vi hinner fylla hela kvarvarande delen av segmentet
    t_used = t_needed_k;
    E_batt = E_seg_max_kWh;
else
    % Vi hinner bara ladda en del av segmentet
    t_used = t_rem_h;
    E_batt = P_batt_k * t_used;  % [kWh] in i batteri
    % Säkerställ att vi inte går över segmentets SoC-slut pga avrundning
    E_batt = min(E_batt, E_seg_max_kWh);
end

% Energi från nätet i detta segment
E_grid = E_batt / eta_tot_k;     % [kWh] från elnätet

% SoC-ökning i detta segment
delta_s_used = E_batt / (f_usable * E_installed_kWh);  % [-]
soc_curr = s1 + delta_s_used*100;                      % [%]

% Klipp mot segmentets övre gräns och max 100 %
soc_curr = min(soc_curr, s_hi);
soc_curr = min(soc_curr, 100);

% Spara segmentdata
t_seg_h(k)        = t_used;
E_batt_seg_kWh(k) = E_batt;
E_grid_seg_kWh(k) = E_grid;

% Minska återstående tid
t_rem_h = t_rem_h - t_used;
```

```
    % Om vi nått 100 % SoC är vi klara
    if soc_curr >= 100 - 1e-6
        break;
    end
end

%% ---- Resultat ----
t_used_total_h   = sum(t_seg_h);          % faktiskt använd laddtid [h]
t_used_total_min = t_used_total_h * 60;    % [min]

E_batt_total_kWh = sum(E_batt_seg_kWh);    % [kWh] lagrat i batteriet
E_grid_total_kWh = sum(E_grid_seg_kWh);    % [kWh] från elnätet

fprintf('Start-SoC:          %.1f %%\n', soc_start);
fprintf('Tillgänglig tid:    %.1f min\n', t_avail_min);
fprintf('Använd tid:         %.1f min\n', t_used_total_min);
fprintf('Slut-SoC:           %.1f %%\n', soc_curr);
fprintf('Energi i batteri:   %.1f kWh\n', E_batt_total_kWh);
fprintf('Energi från nätet:  %.1f kWh\n', E_grid_total_kWh);

% Valfri utskrift segmentvis
disp(table((1:nSeg).', soc_edges(1:end-1).', soc_edges(2:end).', ...
           E_batt_seg_kWh.', E_grid_seg_kWh.', t_seg_h.', ...
    'VariableNames', {'Seg','SoC_lo','SoC_hi','E_batt_kWh','E_grid_kWh','t_h'}));
```

Publicering och arkivering

Godkända självständiga arbeten (examensarbeten) vid SLU kan publiceras elektroniskt. Som student äger du upphovsrätten till ditt arbete och behöver i sådana fall godkänna publiceringen. I samband med att du godkänner publicering kommer SLU även att behandla dina personuppgifter (namn) för att göra arbetet sökbart på internet. Du kan närsomhelst återkalla ditt godkännande genom att kontakta biblioteket.

Även om du väljer att inte publicera arbetet eller återkallar ditt godkännande så kommer det arkiveras digitalt enligt arkivlagstiftningen.

Du hittar länkar till SLU:s publiceringsavtal och SLU:s behandling av personuppgifter och dina rättigheter på den här sidan:

- https://libanswers.slu.se/sv/faq/228316

☒ JA, jag, Haqvin Wedelsbäck har läst och godkänner avtalet för publicering samt den personuppgiftsbehandling som sker i samband med detta

☐ NEJ, jag/vi ger inte min/vår tillåtelse till att publicera fulltexten av föreliggande arbete. Arbetet laddas dock upp för arkivering och metadata och sammanfattning blir synliga och sökbara.